Ref. Ares(2020)646732 - 03/02/2020

EUROPEAN JOINT PROGRAMME FOR THE INTEGRATION OF RADIATION PROTECTION RESEARCH CONCERT

This project has received funding from the Euratom research and training programme 2014-2018 under grant agreement No 662287.

VERIDIC
Validation and Estimation of Radiation skIn Dose in Interventional Cardiology

EJP-CONCERT

European Joint Programme for the Integration of Radiation Protection Research

H2020 – 662287

D9.142 – Dosimeter calibration and measurement uncertainties in Interventional Cardiology

Lead Author: Valentin BLIDEANU

With contributions from: Johann PLAGNARD, Jérémie DABIN, Olivera CIRAJ BJELAC, Joëlle Ann FEGHALI

Reviewer(s): CONCERT coordination team

Work package / Task	**WP 9**	**T 9.9**
Deliverable nature:	**Report**	
Dissemination level: (Confidentiality)	**Public**	
Contractual delivery date:	**Month 56 (January 2020)**	
Actual delivery date:	**Month 56 (January 2020)**	
Version:	**1**	
Total number of pages:	**39**	
Keywords:	**Beam quality, primary standard, dosimeter, calibration**	
Approved by the coordinator:	**Month 57**	
Submitted to EC by the coordinator:	**Month 57**	

Table of Contents

Introduction 4
Uncertainty associated with skin dose measurements 4
Thermoluminescent dosimeters 4
Energy dependence 5
Angular dependence 6
Dose response linearity 6
Dose rate dependence 6
Repeatability 6
Fading 6
Spatial coverage 7
Gafchromic films 7
Quality control dosimeters 11
Selection of relevant beam qualities 13
Establishment of the new reference beams for IC 14
Calibration of dosimeters 15
Quality control (QC) active dosimeters and secondary standard 15
Thermoluminescent dosimeters preparation and reading 16
Calibration settings in the CEA reference beams 16
Dosimeters response 18
Thermoluminescent dosimeters (TLD) 19
Gafchromic films 23
Quality control dosimeters calibrated using secondary standard at VINCA 29
Conclusions 34

Introduction

Various examination techniques are employed in diagnostic radiology using tube voltages from about 20 kV to 150 kV. The tube voltages in fluoroscopy, CT, and dental and general radiography cover the range 50–150 kV, the anode material usually being tungsten. An accurate measurement of dose requires correct calibration of the instrumentation in radiation beam qualities of known properties. In diagnostic and interventional radiology, the specification of radiation qualities is important as the response of all dosimeters depends, at least to a certain extent, on the spectral distribution of the x-rays employed. Radiation qualities are usually specified in terms of the x-ray tube voltage first and second half value layers (HVL).

In order to allow accurate dose monitoring for patients and medical staff in interventional cardiology (IC), the dosimeters must be calibrated prior to their use at the hospital in beam qualities as close as possible to the ones generated by the medical systems. To our best knowledge, before VERIDIC (Validation and Estimation of Radiation skIn Dose in Interventional Cardiology) project there was no primary standard established for the IC, therefore calibration of the dosimeters was done using standard normalized reference X-Ray beams available at the metrology laboratories, resulting in a lower accuracy of the dose measurements during IC since irradiation conditions at hospital were different from the ones used for calibration.

One of the objectives of VERIDIC was to increase the accuracy of dosimeter calibration for IC by establishing appropriate reference X-Ray beam qualities and to provide direct traceability to these beam qualities and so minimize the gap between calibration conditions and configurations used in the clinical environment. This work has been done in the Task 2.1.

Uncertainty associated with skin dose measurements

Skin dose in IC can be assessed by calculations based on exposure and geometrical data supplied by the X-ray equipment or by direct measurements, by placement of a dosimeter on the patients' skin. Nevertheless, there is still no clear consensus about an ideal dosimeter for monitoring surface radiation during IC procedures. The ideal dosimeter should have a response which is linear within the measured dose range, have good angular response and minimally interfere with the image. Dosimeters used in interventional radiology for skin dose assessment are thermoluminescent dosimeters (TLD), radiological and radiochromic films and semiconductor detectors (high sensitivity MOSFET dosimeters and silicon diodes).

Basic properties of these dosimeters are described in this section.

Thermoluminescent dosimeters

Thermoluminescent dosimeters (TLDs) have been used for clinical studies of patient skin dose in interventional cardiology (Kopec et al. 2014, Bogaert et al. 2009, Dabin et al. 2018) for their good dosimetric properties and their tissue-equivalent composition (McKeever et al. 1995, Kron et al. 1998). The most common types of TLDs are LiF:Mg,Ti and LiF:Mg,Cu,P under the form of round or squared pellets with dimensions of few mm. The main sources of uncertainty associated with TLD measurements are the energy dependence, the angular dependence, the dose response linearity, the dose rate dependence, the repeatability and the fading. In addition, the thermal treatment and the reading process of the dosimeters can considerably affect the dosimeter properties and hence the uncertainty sources. Most of those have been thoroughly characterized and described in the scientific literature. A non-exhaustive review focusing on patient skin measurements in IC is presented.

Energy dependence

Several groups have studied the photon energy response of LiF:Mg,Ti and LiF:Mg,Cu,P (Kron et al. 1998, Sáez-Vergara et al. 1999, Olko 2002, Davis et al. 2003, Duggan et al. 2004, Hranitzky et al. 2006, Carinou et al. 2008, Nunn et al. 2008, Parisi et al. 2019); nevertheless, drawing general conclusions remains a challenge because of numerous differences in the study material and methodologies.

Most studies were performed with the N-series beam and Cs-137 or Co-60 as reference and one study also included the RQR-series (Carinou 2008), which is advised as reference for diagnostic applications by the IAEA (2007). Two studies were based on quasi monoenergetic beams (Kron 1998 and Duggan 2004) and one study was performed with the NIST series (Nunn et al. 2008). All authors reported the TLD energy response normalized to the response to high energy photon (Co-60 or Cs-137 or 1 MeV photons in Kron et al. (1998). The description of the beam energy, however, was less homogenous, with some authors using mean energy while others used effective energy. The thermal treatment (pre- and post- irradiation) and the reading protocol of the dosimeters might show great differences between those studies.

Although significant variations can be observed between the studies, the results generally show comparable trends. The dose reponseresponse curves of LiF:Mg,Ti and LiF:MgCu,P are fundamentally different. LiF:Mg,Cu,P usually shows the same shape of energy response in all studies, with a lowest peak around 80-100 keV (Figure 1b). The relative response deviates from ± 20% from unity between 15 keV and 662 keV. However, in few studies the relative response to Cs/Co is always below one, even in the range 30-50 keV (Hranitsky et al. 2006). The results of the energy response among the different studies is more heterogeneous for LiF:Mg,Ti (Figure 1a). The highest peak appears around 30-50 keV. The energy response is up to 40% higher than unity between 15 keV and 662 keV.

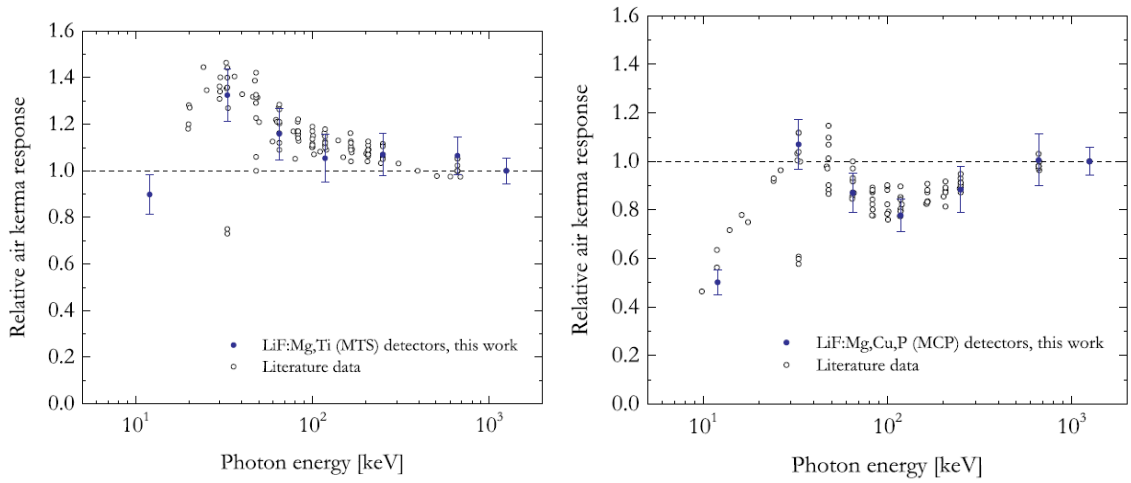

Figure 1: (a) Comparison between the average relative air kerma photon energy response of all LiF:Mg,Ti (MTS) detectors of this study and experimental data from Sáez-Vergara et al. (1999), Olko (2002), Davis et al. (2003) and Hranitzky et al. (2006). (b) Comparison between the average relative air kerma photon energy response of all LiF:Mg,Cu,P (MCP) detectors of this study and experimental data from Sáez-Vergara et al. (1999), Olko (2002), Davis et al. (2003) and Hranitzky et al. (2006). Figure from Parisi et al. (2019).

The different responses might be due to differences in material and in thermal and reading processes. It is also important to mention that some authors used mean energies to report the results while other used effective energy. Nevertheless, from Sáez-Vergara 1999, it appears that different responses of different materials are inherent to the material, not to the reading and annealing procedures, since results from two TL laboratories, with very different procedures, are consistent within experimental uncertainties. This is in agreement with Hranitzky et al. (2006) stating that the annealing and reading processes are expected to have little effect on the relative TLD response as long as the parameters are maintained within a reasonable range during the complete study. Results froOkm Parisi et al. (2019) also support that the lithium isotopic

composition has no visible effect on the energy response. However, from an older literature review performed by Duggan (2004), the energy response of TLD materials might be dependent on the manufacturer of the TLD, the dopant concentration and/or its thermal handling.

Considering photon energies between 15 keV and 120 keV, an energy range which can be encountered in IC, the relative energy response of LiF:Mg, Cu,P deviates with ± 20% from unity between; while for LiF:Mg,Ti, the relative response is up to 40% higher than unity. This will therefore be the dominant source of uncertainty in skin dose measurements in interventional cardiology (IC). Owing to the variation among the TLD energy response in the literature, specific investigation of the complete TLD system, including the thermal treatment and the reading process, is advisable prior to performing measurements in IC. In addition, beams adequately representing the shape of IC spectra should be used in IC (see discussion on the establishment of new reference beam qualities).

Angular dependence

No recent study of angular dependence of LiF:Mg,Ti or LiF:Mg,Cu,P was found in the scientific literature.

Dose response linearity

The dose response of LiF:Mg,Ti might become supralinear at dose levels relevant to IC procedures during which several Gy at the patient skin might be monitored. The onset and degree of supralinearity in the response of LiF:Mg,Ti to photons is a complex mechanism which has been frequently reviewed (for instance McKeever et al. 1995, Gamboa –deBuen et al. 1998 and Massillon-Jl et al. 2006). The supralinearity of LiF:Mg,Ti depends on multiple factors such as the impurity content of the material, the thermal treatment, the reading process and the glow peak temperature. In addition, the degree of supralinearity increases when the photon energy increases.

Unlike LiF:MG,Ti, LiF:Mg,Cu,P shows a linear response over the same dose range (Moscovitch et al. 2007), which is a significant advantage for use in IC.

Dose rate dependence

It is usually accepted that neither LiF:Mg,Ti nor LiF:Mg,Cu,P show dose rate effect. A recent review of the literature for LiF:Mg,Ti, however, concluded there was no reliable experimental evidence supporting the existence or non-existence of intrinsic dose rate effects in the TL response of LiF:Mg,Ti (Horowitz et al. 2018).

Repeatability

No recent study of TLD repeatability of LiF:Mg,Ti or LiF:Mg,Cu,P was found in the scientific literature.

Fading

The fading of the thermoluminescent output signal is a two-components process during which the material gradually loses its capability of producing light following exposure to radiations. The first component is the pre-irradiation fading, which is the loss of the material sensitivity before being irradiated. The second one is the post-irradiation fading, which is the loss of signal after the material has been irradiated (Carinou et al. 2011).

Numerous studies of the fading characteristics of LiF:Mg,Ti and LiF:Mg,Cu,P have been performed during the last decades, with study period from a few days or weeks to more than a year (Bilski et al. 2013), and post-irradiation fading rates ranging from a few % up to tens of % (Moscovitch and Horowitz 2007). Aside from the storage duration and conditions, the fading characteristics depends on various factors such as the material, the radiation type and the thermal and reading processes (Horowitz 1990, Harvey et al. 2010, Carinou et al. 2011).

For LiF:Mg,Ti, wide variation in post-irradiation fading characteristics were observed, from as little as 1% per year to 10% in one month (Moscovitch and Horowitz 2007), depending on the experimental parameters. As early as the seventies, post-irradiation thermal treatments were investigated to limit the amplitude of LiF:Mg,Ti signal fading to a few % (for instance, Burgkhardt and al. 1978a and b). Another approach to limit the fading rate is to perform a glow curve analysis and only use glow peaks that do not fade appreciably, or to integrate glow curves across regions that do not exhibit strong fading (Harvey et al. 2010). Similar rates of decrease in sensitivity were observed for the pre-irradiation fading (Gilvin 2007, Carinou et al. 2011).

In terms of fading, LiF:Mg,Cu,P is usually considered superior to LiF:Mg,Ti for diagnostic medical applications. In a review, Moscovitch and Horowitz (2007) also reported very low post-irradiation fading rates which could be completely removed for storage periods of up to two months at room temperature if an appropriate post-irradiation thermal treatment is performed. However, experimental conditions have again a considerable effect as reported by Harvey et al (2010) in an earlier review of LiF:Mg,Cu,P fading properties. The authors pointed out the wide range of post-irradiation fading encountered in the literature, from non-measurable fading rates (Duggan and Kron. 1999) up to 26% (Hosseini-Pooya and Jafarizadeh 2004) over a 6 monthmonths storage period. Concerning the pre-irradiation fading, a slight increase in the sensitivity, from a few % to 10%, was observed in the first weeks to month after annealing, followed by a decrease till reaching the initial value (Carinou et al. 2011).
As for the energy response, each dosimetry service should therefore study the fading effect for its own material, thermal treatment and reading processes since these parameters can affect the fading rate.

Spatial coverage

Aside from their dosimetric properties, an additional uncertainty may arise from the detectors' limited spatial coverage when they are used for detecting the maximum dose in a radiation field with an heterogeneous dose distribution, as monitoring the maximum skin dose (MSD) during interventional procedures. Indeed, it might be very challenging to predict where the MSD will occur and to know whether it was actually recorded. Depending on the number of TLDs used, the size of the MSD region and the dose gradients on the patient skin, the probability of not detecting the MSD might be high. and dominate the other sources. For instance, in a study including 68 IC procedures, only 63% of the maximum skin dose could be measured on average with a grid of 40 TLDs covering the patient back (Dabin et al. 2015).

Gafchromic films

Large-area radiochromic films (Gafchromic XR type T, for viewing in transmitted light and R, for viewing in reflected light) are intended for the measurement of skin dose in high dose procedures. They are made of nearly tissue equivalent material and are of the size 35 cm x 42 cm. When exposed to radiation, their color changes proportionally to the dose received. The sheets could be quantitatively analyzed with appropriate software after digital scanning (Farah *et al.* 2015). The reliability and applicability of GafChromic films for quantitative estimates of skin dose in interventional cardiology is directly related to film properties and performance in clinical conditions (Greffier et al. 2017, Didier et al. 2019). Uncertainties related to the use of such films for patient skin dose assessment in the interventional environment have been extensively addressed in the literature. Specifically, for XR-Type R GafChromic films, great effort has been invested to determine their dosimetric characteristics in terms of film uniformity, dose linearity, dose fractionation, post-exposure density growth, energy dependence, dose-rate dependence, storage lighting, and UV light sensitivity. However, contradictory results can be found in the literature (Ciraj Bjelac et al 2019).

Therefore, basic dosimetric properties and factors contribution to the overall uncertainty of skin dose assessment with relation to the use of the radiochromic films are discussed extensively in this report.

Energy dependence

Although McCabe et al. (2011) studied the energy dependence of XR-RV3 film covering the entire interventional energy range (from 60 to 120 kV, half value layers (HVL) ranging from 1.68 to 6.96 mm Al), the considered X-ray beam qualities are not fully close to clinical beam qualities. According to McCabe et al. (2011), the energy dependence of XR-RV3 film decreased as the air kerma level increased. The white-facing exposures showed larger energy dependence than the orange-facing case. Per manufacturer's information for XR-RV2 radiochromic film, between 80 and 120 kVp fluoroscopic beam qualities, the difference in film darkening for a dose of 500 cGy was expected to be less than 8%. However, McCabe et al. (2011) concluded that difference between the UW80-M and UW120-M beam qualities at 500 cGy air kerma for orange-facing exposures was 7.0%. For the white-facing exposures, the difference was 9.4%.

In the work of Farah et al (2015), films were irradiated to a dose of 0.5 Gy using different standard beam qualities (RQR5, RQR9, A, B and C series). The films showed lower mean pixel values when irradiated with beams of higher quality (kV or filtration). The difference on film darkening increases with the change in radiation quality reaching up to 15 % for the C-120 beam, compared to RQR5 beam quality (Farah *et al.* 2015). Furthermore, in this work for yellow side irradiations, up to 4 % difference on pixel value was registered for RQR4 vs. RQR6 beams and up to 13 % for RQR4 vs. RQR9 beams. White side irradiations showed higher values (up to 8 % for RQR4 vs. RQR6 and up to 20 % for RQR4 vs. RQR9), which is in agreement with data by McCabe et al. (2011).

Farah et al. (2015) analyzed the variation of film response as a function of dose for the two clinical beams of medium (75 kV, AVL4 mm Al) and high (120 kV, 6 mm Al) energy. A maximum 9% difference on film reading was observed for the same dose delivered by a medium or a high energy clinical beam. For the dose range examined in this study, film response appears to be dose independent. Similar findings were observed for films irradiated to 0.3 Gy with tube voltage or additional copper filtration covering the entire possible clinical range. A higher variability of film response as a function of radiation quality for white side film exposures when compared to yellow side irradiations was demonstrated in this work. From the result, and considering the clinical beams regularly used on current x-ray systems (60–120 kV, HVL 2.46–7.75 mm Al), it can be concluded that film response variation with radiation quality is limited to within 6–8 %. Yellow side film exposure positively contributes in reducing this uncertainty (Farah *et al.* 2015).

Dose rate dependence

In interventional procedures, clinical conditions involve backscatter radiation and use high-dose rate pulsed beams while laboratory beams are typically free in- air, continuous, and of low dose rate. Therefore, the film characterization under clinical conditions is needed. In addition, batch-to-batch film behavior needs to be checked. In addition, Farah et al. (2015) assessed the performance of multiple and commonly used scanner models that may have an impact on the accuracy of the skin dose assessment (Farah *et al.* 2015).

In this work films were irradiated in laboratory conditions using RQR5 beam and different dose rates: 3.5, 10, 20, 40, 60 and 100 mGy/min and in relevant clinical beams and acquisition modes (fluoroscopy, cineangiography and Digital Subtraction Angiography) at dose rates of 1.9 mGy/min, 340 mGy/min and 1080 mGy/min, respectively. In addition, films were irradiated at 80 kV and HVL of 3.45 mm Al, with set tube current at 10, 50, 100, 200 and 400 mA (Farah *et al.* 2015).

In laboratory conditions, when compared with irradiations with the lowest dose rate of 3.5 $mGymin^{-1}$, films have a response variability within 4.2% for laboratory dose rates of up to 100 $mGymin^{-1}$. This result was also confirmed for films characterized in clinical conditions, as film darkening did not differ by more than 4.9% with dose rates ranging from 1.9 mGy min^{-1} to 1080 $mGymin^{-1}$ and yellow side exposures. Higher values were observed for white side film exposures with up to 10 % difference on film reading. This null effect of dose rate and pulse rate on film darkening may be reasonably explained by the slow

polymerization process of GafChromic films. McCabe *et al*. (2011) reported that the XR-RV3 manufacturer indicates a dose rate dependence <3 % between 0.03 Gy min^{-1} and 3 $Gymin^{-1}$, in agreement with above described findings.

Other film-related uncertainties

In addition to the above mentioned properties of gafchromic films, Farah et al. (2015), investigated film-to-film uniformity, film darkening over time, impact of scanner used and impact of fitting parameters (Farah *et al.* 2015).

Film-to-film uniformity

Two types of uniformity test were performed by Farah et al. (2015). For all film pieces and participating centers, single film uniformity also known as intra-sheet uniformity was calculated using the coefficient of variation (COV) value. Meanwhile, the batch-to-batch variability, i.e. inter-sheet uniformity, was determined by comparing the response of XR-RV3 film pieces of 3 different batches.

The COV was used to determine the film-to-film uniformity in one batch. Film pieces from all centers were found to have an intra-sheet uniformity within 0.5 % better than literature findings for other film types (Richley *et al.* 2010). Nonetheless, results of the extensive tests on multiple batches in both laboratory and clinical settings shows that XR-RV3 film-to-film uniformity is satisfactory and dose-independent. These findings are lower than the 2.5% (k=1) film uniformity uncertainty determined by McCabe *et al.* (2011) and confirm manufacturer's indications on film uniformity in one batch (<5%). Meanwhile, the batch-to-batch variation of XR-RV3 film was found to be within 7 % for non-irradiated films and within 24 % for films irradiated to a dose of 4 Gy using the RQR6 beam quality. In the latter case, the readout difference is lower when comparing reflectance (within 7 %) further highlighting the need for background normalization. Nonetheless, these values are high, indicating that each new batch must be calibrated separately (Farah *et al.* 2015).

Films from different batches were found to continue to darken with time after exposure, but generally stabilizing 24 hours post-irradiation for both laboratory and clinical beam qualities. The largest difference on reflectance between the 1 h post-irradiation reading and the 24 h reading was within 3%. In addition, film darkening analysis showed no dependence on the dose level (0–10 Gy) or on exposure side (yellow or white). Finally, analysis showed little effect (<1.5 %) of repetitive reading, i.e. UV light, even during the early stages of the polymerization process (Farah *et al.* 2015). These results are in agreement with McCabe et al. (2011) who noticed that the signal changes most dramatically for the first 8 hours and less noticeably thereafter. Farah et al. (2015) concluded that 24 hours reading interval recommended by the manufacturer is appropriate for XR-RV3 films.

Extensive analysis of fit functions used for the calibration of XR-RV3 gafchromic films and impact of scanner to the overall uncertainty of ski dose assessment is described elsewhere (Farah *et al.* 2015, McCabe *et al.* 2011).

Furthermore, scanner-related uncertainty analysis showed that multiple scanner models and types can be used for such dosimetry applications. However, the performance of the scanner may vary from one model to another and scan uniformity and long-term stability need to be checked prior to film readings. Scanner readings were found to be mostly affected by the long-term stability of the scanner with up to a 3.6 % difference between two weekly readings. To compare scanner-to-scanner readings, background normalization was shown to be mandatory. The overall scanner-related uncertainty was found to range from 2 % to 7 % at one standard deviation (Farah *et al.* 2015).

In general, calibration curves showed a strong dependence on film orientation (white side versus orange side facing the x-ray source) and tube voltage and small dependence on patient-equivalent backscattering

(McCabe *et al.* 2011). Different equations available in the literature were tested as part of the fitting-related uncertainties (Farah *et al.* 2015). The results have shown that exponential fits could not correctly reproduce XR-RV3 response. Meanwhile, easy to use third order polynomials provided appropriate fitting quality but suffered from having the highest dependence on fit parameters. As such, fitting uncertainties were found to be the main source of uncertainty when determining skin dose using XR-RV3 GafChromic films.

Overall uncertainty

A method to determine the overall uncertainty associated with the use of XR-RV3 Gafchromic films to assess skin dose in interventional radiology is extensively described elsewhere (Farah *et al.* 2015, EURADOS 2019, Greffier et al. 2017). The uncertainty differs for three foreseeable exposure scenarios, depending on the level of control of measurement conditions (A- tightly controlled measurement conditions, B-well-defined laboratory calibration is performed and parameters related to clinical application of dosimetry films are less controlled, C- conditions of exposure, film handling and readout are weakly controlled). As described in Table 1. the lowest possible relative combined standard deviation at about 5 %, but it can reach even 40% in the weakly controlled conditions(k=1), highlighting the need for careful processing of film dosimetry steps.

Influence quantity/parameter	***Scenario A***	***Scenario B***	***Scenario C***
	(%)	***(%)***	***(%)***
Dose delivery uncertainty			
Air kerma rate measurements	0.8	2.6	5
Setup error and film positioning	0.1	0.5	1
Beam uniformity	0.3	2	5
Backscatter radiation	-	5	10
Scanner-related uncertainties			
Scan uniformity	0.3	0.7	2
Short term stability	0.1	0.7	2.5
Long term stability	1.5	2.2	3.6
Scanner readout, warm-up and software effects	-	2.5	5
Uncertainties related to a film			
Inter/intra batch uniformity	1	4	7
Darkening over time	0.5	1.5	3
Effect of scan light	0	1	1.4
Dose rate dependence	1	3	5
Radiation quality dependence	2	10	15
Film orientation	0	6	10
Humidity and temperature during transportation and storage	0	2	5
Uncertainties related to calibration			
Fitting equation	2	6	10
Dose range of calibration points	2	10	22
Number and distribution of data points	2	8	17
Reading outliers and precision of fit parameters	3	10	20
Relative combined standard uncertainty (k=1)	5	20	39
Relative expanded uncertainty (k=2)	9	41	78

Table 1: Summary of skin dose assessment uncertainty using XR-RV3 Gafchromic films (adopted from Farah et al. 2015, EURADOS 2019).

As described above, there are different sources of uncertainties arising from the film (inter/intra-batch uniformity, scan light effect, reading ROI size, beam uniformity, dose rate and beam quality and backscatter dependence) and the scanner (warm-up, uniformity, short/long term stability) properties (Farah *et al.* 2015, McCabe *et al.* 2011). However, Habib Geryes et al. (2018), investigated additional sources of uncertainties, as impact of film irradiation during the polymerization process and storage conditions (recommended dark storage conditions, daylight conditions, humid and low temperature conditions). These proved to introduce non-negligible contribution to the overall measurement uncertainty (2.1% prolonged irradiation effect and 3.2% for storage conditions) while calibration beam quality (6.1%) and backscatter radiation (8.1%) remained the main sources of uncertainties. The overall measurement uncertainty was estimated to be within 22.8% (k=2) (Habib Geryes et al. 2018)

Quality control dosimeters

Various examination techniques are employed in diagnostic radiology using tube voltages from about 20 kV to 150 kV. The tube voltages in fluoroscopy, CT, and dental and general radiography cover the range 50–150 kV, the anode material usually being tungsten. An accurate measurement of dose requires correct calibration of the instrumentation in radiation fields of known properties. In diagnostic radiology, the specification of radiation qualities is important as the response of all dosimeters depends, at least to a certain extent, on the spectral distribution of the x-rays employed. Radiation qualities are usually specified in terms of the X ray tube voltage first and possibly HVL second**.**

Ionization chambers have been the standard instruments used for diagnostic radiology dosimetry and quality assurance for many years. Dosimeters based on semiconductor technology are now becoming widely available, and as the semiconductor detectors are smaller, they are more convenient to use in many situations. Diagnostic dosimeters should be in compliance with IEC 61674 standard (1997), which applies both to dosimeters equipped with ionization chambers and to semiconductor detectors. Traditionally, the main disadvantage of these devices has been their energy dependence of response which differs considerably from that of ionization chambers.

Semiconductor diodes do not inherently have response which is relatively constant with photon energy in the diagnostic X-ray range for measurement of air kerma, which is a feature of ion chambers. In order to improve energy dependence, multiple semiconductor elements are incorporated into the semiconductor detector used for X-ray dosimetry in order to make an assessment of radiation quality that is used to derive a dose correction compensation, which is then applied automatically.

The commercial semiconducting detectors are mounted on lead backing plates, to attenuate radiation incident from the rear. This is required to ensure that the radiation incident on the detector elements represents that transmitted through filters at the front of the detector in order to ensure that the automatic energy compensation is applied correctly. As a result, it is the air kerma incident from the direction of the primary beam that is measured. Nevertheless, these types of detectors have found many applications in routine clinical measurements in hospitals. Most of them are capable to measure the air kerma, tube voltage, half value layer (HVL), and exposure time, as well as the output waveform from a single irradiation.

Martin (2007) proved that dosimeters for x-ray equipment QC based on semiconductor detectors (SDs) provide a viable alternative to ion chamber (IC) based dosimeters. The responses of semiconductor detectors (SDs) and ICs to x-ray beams with a variety of radiation qualities have been measured in order to assess differences in response. Measurements have been made with experimental arrangements simulating use of the detectors in performance testing of digital radiography and fluoroscopy equipment. Results show that differences in photon energy responses between the detectors are small, but because ICs are sensitive to radiation incident from all angles, they record more scattered radiation than SDs. It was concluded that SDs are more appropriate for measurements of image receptor doses and are recommended for setting up automatic exposure control devices for digital radiography. ICs are suitable

for assessment of patient entrance surface dose rate measurements. Correction factors that could be applied to allow comparisons between measurements with different dosimeters are proposed.

Both ICs and SDs are useful instruments for measuring air kerma levels in x-ray beams. Their performance is comparable for measurements made free in air, but measurements recorded when radiation scattered from nearby objects is present may be significantly different. Although the ideal would be to perform all measurements free in air, if dosimeters are to be used for setting up AEC devices for digital radiography or measuring entrance surface dose rates at the faces of image intensifiers and at phantom surfaces during fluoroscopy, then consideration must be given to how these measurements should be performed. The results in this study have shown that differences in measurements recorded by ICs and SDs are related to the amount of scatter in the radiation field and are due primarily to the different angular sensitivities of the detectors. The amount of scatter depends on both the position at which any measurement is made and the size of the field used. Martin (2007) formulated the recommendations on which type of dosimeter to use when making different measurements, and correction factors that may be applied when other types of dosimeter (Martin, 2007). For example, for the patient dose measurement in fluoroscopy, IC is more suitable, as dose rate measured using SD should be multiplied by 1.25. For measurement of dose rate at image intensifier level, both types of detector can be used. In radiography, SD is more suitable detector and if IC is used the reading of IC shall be multiplied by 0.75 (Martin, 2007).

An overall error of 7% in dose determination is acceptable in diagnostic radiology (IAEA 2007). IEC 61674 standard (IEC 1997) provides the limits for the variation in response of diagnostic radiology dosimeters. Dosimeters that comply with the IEC standard should measure the air kerma and the air kerma rate with ±5% accuracy at reference conditions. However, under non-reference conditions, influence quantities, like beam quality, air kerma, air kerma rate, and irradiation conditions, could increase the total measurement uncertainty beyond 5% (Hourdakis at al. 2010). This highlights the importance of investigating dosimeters' air kerma dependence of response for these exposure conditions.

Furthermore, factors as direction of incident radiation, extra focal radiation and scattered radiation, especially in cases when it emerges from tissue equivalent phantoms, could introduce significant errors and could increase the uncertainty of the measurement high enough to push the dosimeters outside of the acceptable range (IAEA 2007, Martin 2007).

As explained above, depending on the application, a dosimeter might be subjected to beam qualities from 20 kV to 150 kV and dose rates from µGy/sec to Gy/sec. Clinical irradiation conditions are not always equivalent to calibration conditions and this will have an effect on the result of the measurement. In fact, standard calibration laboratories could provide neither radiographic nor fluoroscopic irradiation similar to that at clinical. Consequently, in calibrations of dosimeters operating in "dose rate" mode, the applied x-ray tube current (and subsequently the air kerma rate) is often higher than that of clinical fluoroscopy systems, where the dosimeter is used. Likewise, calibrations of dosimeters operating in integrating mode are often performed at tube currents and air kerma rates much lower than those applied in clinical radiography (Hourdakis et al. 2010).

Energy dependence

IEC standard 61674 (IEC 1997) imposes ±5% upper limit of variation of response at the 50 kV—150 kV range. The results of extensive testing of different types of dosimeters, including both SD and IC, showed that all dosimeters being tested complied with the ±5% IEC limit. Although, semiconductors have generally a more pronounced energy dependence of response, modern solid state detectors (Piranha and Unfors) showed a flat energy dependence of response (less than 2%). Tested ionizing chambers showed greater variation in energy response (1%-4%), so appropriate calibration coefficients and correction factors should be applied (Hourdakis et al. 2010).

Angular response

IEC standard 61674 (IEC 1997) imposes ±3% upper limit of variation of response of dosimeters in the range of angles of ±5 degrees from the reference direction (IEC 1997). Yet, some of the recently tested dosimeters showed an asymmetric angular response which respectively under- and overestimated the dose contribution from the rear and lateral directions by the same amount of 50% (Tse and McLean, 2015).

Air kerma rate dependence and response at different irradiation conditions

Different irradiation conditions, like x-ray tube design, x-ray operational mode (radiographic or fluoroscopic), air kerma rate, as well as the dosimeter's operational mode (integrating or dose rate) did not affect significantly the response of a dosimeter. The dosimeters being tested in this study showed performance characteristics within the IEC standard and could measure the dose with less than 5% error.

Based on the available literature data, one may conclude that a dosimeter that complies with IEC standards and operates according to its specifications could be used at typical clinical exposures conditions taking into account only corrections for the energy dependence of response. Nevertheless, the user should investigate a dosimeter's response and performance at various exposures conditions at clinical beam. (Hourdakis et al. 2010).

Selection of relevant beam qualities

An inventory of the X-Ray generators configurations (tube voltage (kVp) and added filtration (mmAl and mmCu) used by the different IC systems has been established by the partners of the project. Hundred-eighty RDSRs were collected from 6 systems of the four main vendors (2 General Electric (GE), 2 Siemens, 1 Philips and 1 Canon systems) from France, Italy, Ireland and Switzerland; 30 RDSRs were collected for each system. Every RDSR was first analyzed according to the frequency (%) of combinations of tube voltage and added filtration used during the IC procedure; fluorography and fluoroscopy modes were analyzed separately. The 30 RDSRs from each angiographic system were then used to draw two histograms, representative of the tube voltage – added filtration used by the system in fluoroscopy and in fluorography. The different imaging approaches implemented by the vendors result in a wide range of tube voltage (from 60 to 120 kVp) and added filtration (from 0 to 0.9 mmCu). Nevertheless, it appeared from a visual inspection of the histograms, that limited combinations of tube voltage and added filtration could satisfactorily represent the different systems. A first set of eight configurations, all of them using a tungsten anode oriented at an angle of 10^0 with respect to the direction of electrons and an inherent filtration with 2.5 mm of aluminum was selected. based on these considerations. The X-Ray spectra emitted for these eight configurations have been calculated using the code SpekCalc, a commonly used and extensively validated tool for applications using X-Ray tubes (G. Poludniowski et al. 2009). The results are presented in Figure 2.

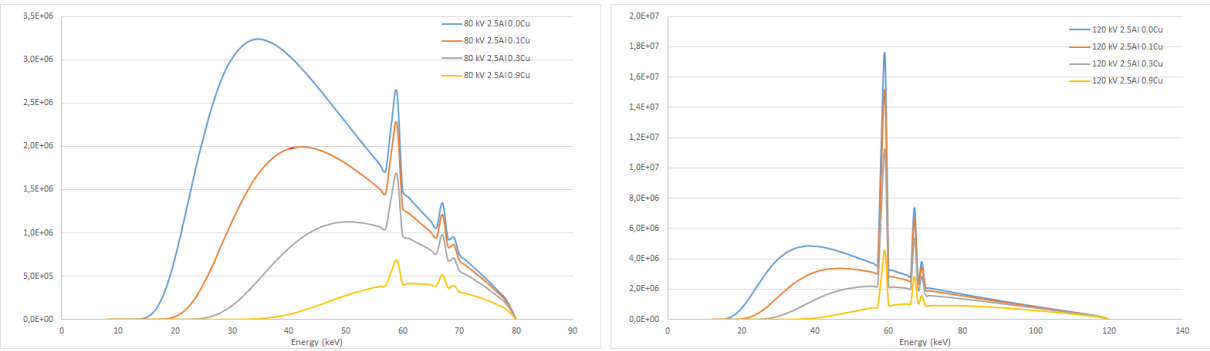

Figure 2: Spectra for eight X-ray tubes configurations used in IC

These first results allowed to compare the X-Ray spectra produced by the eight configurations and due to the similarity observed, to reduce the number of beam qualities to be further studied to four (blue and yellow spectra in Figure 1), two for each 80 and 120 kV voltages corresponding to the extreme conditions in terms of X-Ray filtration (without any and with maximum copper filtration with a thickness of 0.9 mm).

Establishment of the new reference beams for IC

CEA has developed during the past years a reliable method using CdTe semiconductor detector and appropriate correction algorithms to accurately measure the spectra emitted by the X-Ray tubes (J. Plagnard 2014). Based on this method, the spectra emitted by the conventional X-Ray generators available at CEA can be measured and compared with the spectra specific to different applications. By iterative filtrations it is possible to reproduce with conventional generators the beam qualities for a given application, in this case interventional cardiology (IC). A presentation of the set-up used is given in Figure 3.

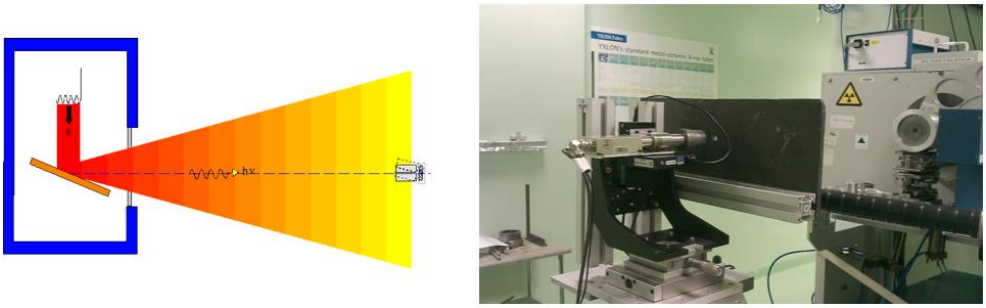

Figure 3: Schematic representation of an X-Ray tube with emitted beam and positioning of the spectrometry detector (left). The experimental set-up used for the measurement of the spectra of the beams emitted by one of CEA's X-Ray generators (right)

In this way, the previously selected more relevant four beam qualities for the IC have been reproduced at CEA using a conventional Siefert 320 X-Ray generator. The Figure 4 shows the very good agreement achieved between the measured spectra and the ones calculated using SpekCalc code.

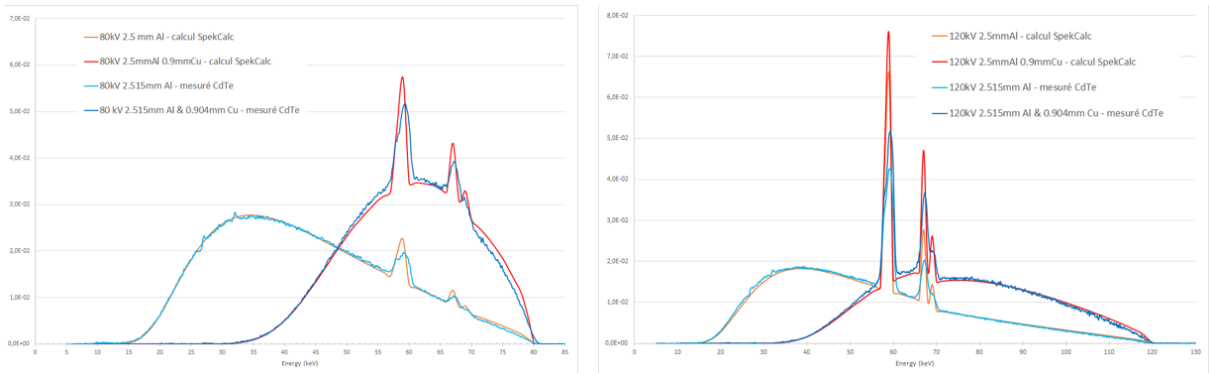

Figure 4: Validation by spectrometry of the beam qualities established using CEA's conventional Siefert 320 X-Ray tube reproducing the four selected qualities for the IC

The new beams established by CEA have been further metrologically characterized in terms of air kerma (K_{air}) rate, the reference quantity for the applications using X-ray beams. The primary standard used was a free-air ionization chamber, an instrument manufactured by CEA allowing the absolute measurement of the K_{air} rate for each beam quality (Figure 5) (W. Ksouri 2008).

Four new reference beams dedicated to interventional cardiology have been established in this way, allowing further calibration of the measurement devices used at the hospital to monitor the doses received during the interventions. In addition to these new IC specific beam qualities, another normalized, well-known beam quality already available at CEA (RQR8 described in the international standard ICE 61267) has been considered for the calibration. This beam quality being close to the new ones in terms of energy spectra (Figure 6), it allows a confidence check by comparing the calibration results between the new and the existing normalized conditions.

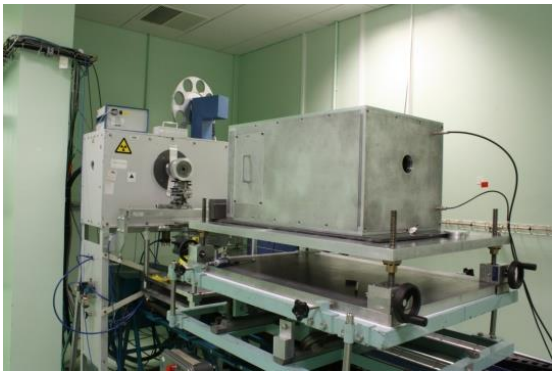

Figure 5: The primary instrument (free-air ionization chamber) in front of the X-Ray generator used for the absolute measurement of the reference quantity K_{air} rate for each beam quality

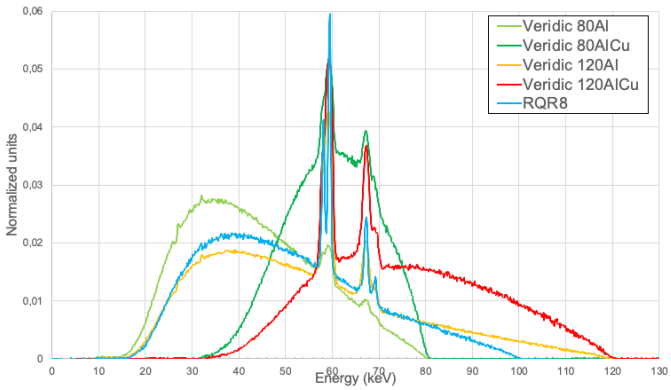

Figure 6: Energy spectra for the four new normalized IC beam qualities compared to the normalized RQR8 beam

Calibration of dosimeters

Quality control (QC) active dosimeters and secondary standard

Three types of solid-state active dosimeters (Figure 7) frequently used in clinics for quality control (QC) measurements to be calibrated in the new reference beams established by CEA using its primary standard have been selected by the VERIDIC partners as being the most relevant for the dose monitoring in clinical conditions.

Figure 7: The three types of dosimeter calibrated in the new reference beams for interventional cardiology.

In addition, TLD and Gafchromic film type passive dosimeters have been irradiated in the new reference beams of CEA at very precise air kerma values to study their response as a function of air kerma rate, energy and angle of incidence of the X-Ray beam.

Finally, one ion chamber EXRADIN MAGNA A600 has been calibrated by CEA to serve as secondary standard for additional calibrations at the VINCA institute. These calibrations are described in the section "Quality control dosimeters calibrated using secondary standard at VINCA".

Thermoluminescent dosimeters preparation and reading

All TLDs were LiF:Mg,Cu,P material (MCP-N, Institute of Nuclear Physics, Poland). Those were circular pellets of 4.5 mm diameter and 0.9 mm thickness. Sets of 3 dosimeters were prepared for each irradiation setting. Before exposure, the TLDs were annealed 10 minutes in an oven at 240°C, followed by a fast cooling in a freezer at -10°C. Two sets of 4 TLDs were used to monitor the dose accumulated during storage and transportation. After exposure and before read-out, the dosimeters were heated at 120°C in an oven for 30 minutes. The TLDs were read on a Harshaw 5500 system with a constant rate of 10 °C/s from room temperature up to 240°C. TLD signal output was corrected for the individual sensitivity of each dosimeter, which was determined using a Cs-137 source.

Calibration settings in the CEA reference beams

The table below gives an overview of calibration conditions for the active QC dosimeters according to the protocol established and agreed within the project.

The active dosimeters have been calibrated for the four new IC beam qualities (VERIDIC1 to 4) as well as in the RQR8 normalized beam at air kerma rates between 0,04 and 0,4 mGy/sec. In order to study the influence of the air kerma rate on the dosimeters response they have been also calibrated at higher air kerma rates around 1,3 mGy/sec for three out of the five beam qualities.

Beam quality	HV (kV)	Mean energy (keV)	Absolute air kerma rates		
			µGy/s	Uncertainty (%)	mGy/min
RQR8	100	50.8	387.790	0.32	23.267
VERIDIC1 80Al	80	43.24	314.130	0.32	18.848
VERIDIC2 120Al	120	54.58	321.000	0.34	19.260
VERIDIC3 80AlCu	80	60.01	44.365	0.38	2.662
VERIDIC4 120AlCu	120	74.53	247.370	0.31	14.842

Beam quality	HV (kV)	Mean energy (keV)	Absolute air kerma rates		
			mGy/s	Uncertainty (%)	mGy/min
RQR8	100	50.8	1.3533	0.31	81.198
VERIDIC1 80Al	80	43.24	1.3308	0.31	79.848
VERIDIC2 120Al	120	54.58	1.2750	0.31	76.500

Table 2: Calibration conditions for the active QC dosimeters in the reference beams established by CEA.

The irradiation configurations for the passive TLD and Gafchromic films are given by the protocol established by the project as shown in the following tables. A total number of 81 TLD and 94 Gafchromic film dosimeters were used for this study and the complete results have been provided to the project partners. The dosimeters have been irradiated at a reference value for the time integrated air kerma and for several air kerma rates (5, 15, 25, 35, 50, 70, 100, 140 mGy/min).

TLD number	Beam	Tube voltage (kV)	I (mA)	Angle (°)	irradiation time (sec)	Air-kerma (mGy)	Uncertainty (% k=1)
1,2,3	RQR8	100	4	0	181.17	70.22	0.34
76,77,78	VERIDIC1 80Al	80	4	0	223.18	70.04	0.34
7,8,9	VERIDIC3 80AlCu	80	10	0	225.18	10.00	0.41
10,11,12	VERIDIC2 120Al	120	2	0	218.18	69.94	0.34
13,14,15	VERIDIC4 120AlCu	120	10	0	283.19	70.08	0.34

TLD number	Beam	Tube voltage (kV)	I (mA)	Angle (°)	irradiation time (sec)	Air-kerma (mGy)	Uncertainty (% k=1)
16,17,18	RQR8	100	4	15	181.18	70.23	0.60
19,20,21				-15	181.18	70.23	0.60
22,23,24				30	181.18	70.23	0.60
25,26,27				-30	181.18	70.23	0.60
28,29,30				45	181.18	70.23	0.60
31,32,33				-45	181.18	70.23	0.60
34,35,36				60	181.18	70.23	0.60
37,38,39				-60	181.18	70.23	0.60
40,41,42				90	181.18	70.23	0.60
43,44,45				-90	181.18	70.23	0.60
46,47,48	VERIDIC3 80AlCu	80	10	15	225.19	10.00	0.65
49,50,51				-15	225.19	10.00	0.65
52,53,54				30	225.19	10.00	0.65
55,56,57				-30	225.18	10.00	0.65
58,59,60				45	225.19	10.00	0.65
61,62,63				-45	225.18	10.00	0.65
64,65,66				60	225.18	10.00	0.65
67,68,69				-60	225.18	10.00	0.65
70,71,72				90	225.18	10.00	0.65
73,74,75				-90	225.19	10.00	0.65

TLD number	Beam	Tube voltage (kV)	I (mA)	Angle (°)	irradiation time (sec)	Air-kerma (mGy)	Uncertainty (% k=1)
58,59,60	RQR8	100	0.9	0	840.20	73.970	0.33
61,62,63			2.6	0	280.19	70.737	0.33
64,65,66			4.3	0	168.18	70.065	0.34
67,68,69			6	0	120.18	69.855	0.36
70,71,72			8.6	0	84.18	70.082	0.39
73,74,75			12	0	60.18	69.863	0.44
76,77,78			17.2	0	42.17	70.095	0.52
79,80,81			24.1	0	30.17	70.215	0.65

film number	Beam	Irradiation time (sec)	Air-kerma (mGy)
1,2	RQR8	51.17	100.43
3,4		127.18	249.60
5,6		204.19	400.74
7,8		357.20	701.04
9,10		433.20	850.20
11,12		510.21	1001.34
13,14		764.21	1499.84
15,16		1019.22	2000.32
17,18		1274.22	2500.78
19,20		1528.22	2999.28
21,22		1783.23	3499.77
23,24		2548.24	5001.18

film number	Beam	Irradiation time (sec)	Air-kerma (mGy)
25,26	VERIDIC1 80Al	63.18	100.254
27,28		158.19	251.016
29,30		252.19	400.175
31,32		441.20	700.096
33,34		535.20	849.255
35,36		630.20	1000.001
37,38		945.22	1499.875
39,40		1260.21	1999.701
41,42		1575.22	2499.559
43,44		1891.22	3000.988
45,46		2206.22	3500.830
47,48		3151.23	5000.372

film number	Beam	Irradiation time (sec)	Air-kerma (mGy)
49,50	VERIDIC2 120Al	31.17	100.601
51,52		77.18	249.098
53,54		124.18	400.791
55,56		217.19	700.981
57,58		263.19	849.446
59,60		310.19	1001.138
61,62		465.20	1501.433
63,64		620.21	2001.728
65,66		774.22	2498.795
67,68		929.21	2999.025
69,70		1084.21	3499.288
71,72		1549.21	5000.075

film number	Beam	Irradiation time (sec)	Air-kerma (mGy)
89,90	VERIDIC3 80AlCu	1080.21	100.025
91,92		2700.23	250.036
93,94		4319.24	399.953

film number	Beam	Irradiation time (sec)	Air-kerma (mGy)
73,74	VERIDIC4 120AlCu	195.19	99.764
75,76		489.20	250.035
77,78		782.21	399.795
79,80		1369.22	699.822
81,82		1663.21	850.083
83,84		1956.22	999.844
85,86		2934.22	1499.709
87,88		3913.23	2000.091

Table 3: Irradiation conditions for the passive dosimeters in the reference beams established by CEA.

Dosimeters response

Quality control dosimeters calibration using the primary standards of CEA

The complete calibration and irradiation results have been provided to the consortium as official certificates for each device.

An example of the results for the five beam qualities is given in Figure 8 for the active QC dosimeters at air kerma rates ranging from 0,04 to 0,4 mGy/sec. Considering the RAYSAFE X2 and the RADCAL AGMS-DM+ dosimeters, one can observe that the calibration factor is relatively constant with the mean energy of the beam and that there is a good agreement for the calibration factor between the new reference beam qualities and the normalized RQR8 beam.

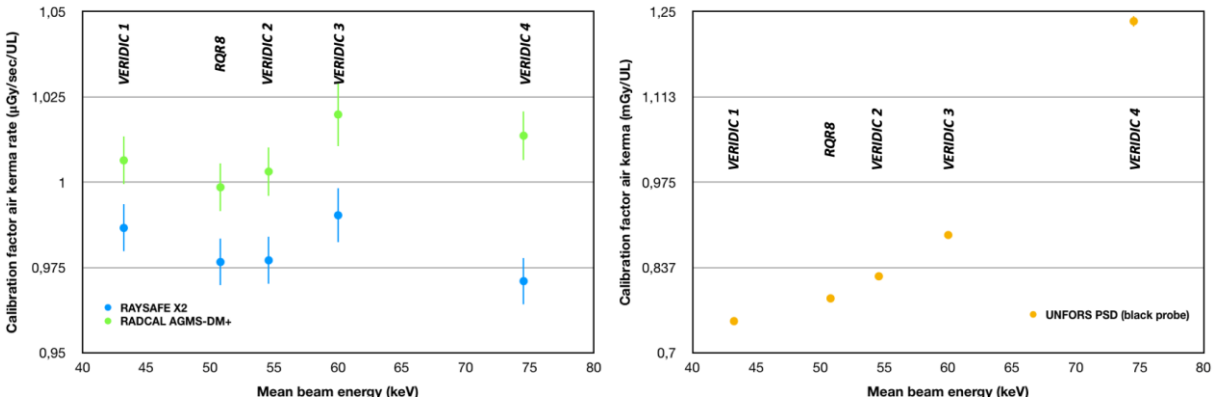

Figure 8: Calibration factors for the active QC dosimeters obtained for the interventional cardiology dedicated reference beams and for reference air kerma rate values ranging from 0,04 to 0,4 mGy/sec.

On the contrary, the semiconductor-based dosimeter UNFORS PSD has a response that shows a strong dependency with the mean energy of the beam.

No significant influence of the air kerma rate on the dosimeters response has been found for three of the beam qualities studied. Figure 9 shows almost identical values for the calibration factors at a refence air kerma rate of the order of 1,3 mGy/sec as the ones in Figures 7 measured as much lower rates.

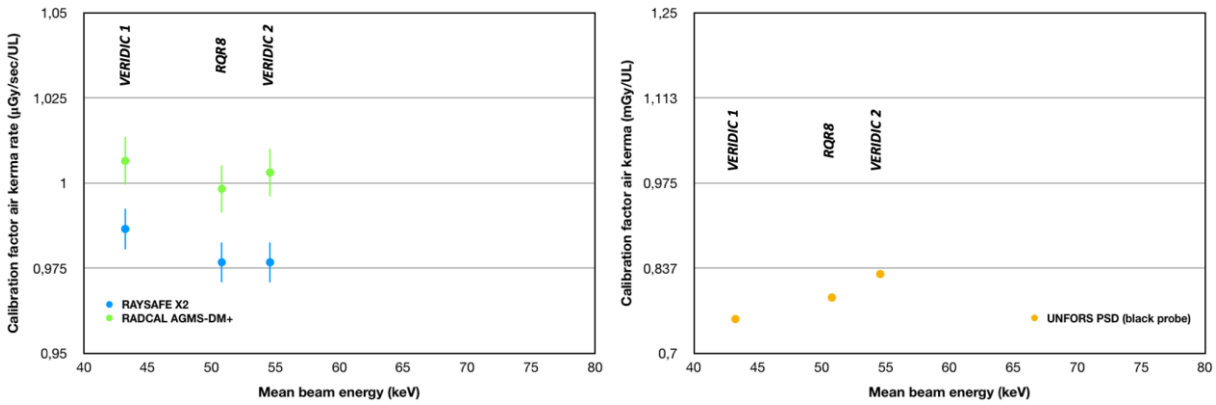

Figure 9: Calibration factors for the active QC dosimeters obtained for the interventional cardiology dedicated reference beams and for reference air kerma rate values around 1,3 mGy/sec.

Thermoluminescent dosimeters (TLD)

The results of the dose rate dependence test are presented in Figure 10. Each point represents the average response of three dosimeter; for each irradiation setting, the coefficient of variation between the three TLDs was no more than 5%. Results are normalized to the response at 5 mGy/min. TLD response varies between -1 and 2%. Those results are smaller than the variation of the response of a TLD set, and within the measurement uncertainty. No dose rate effect can therefore be inferred.

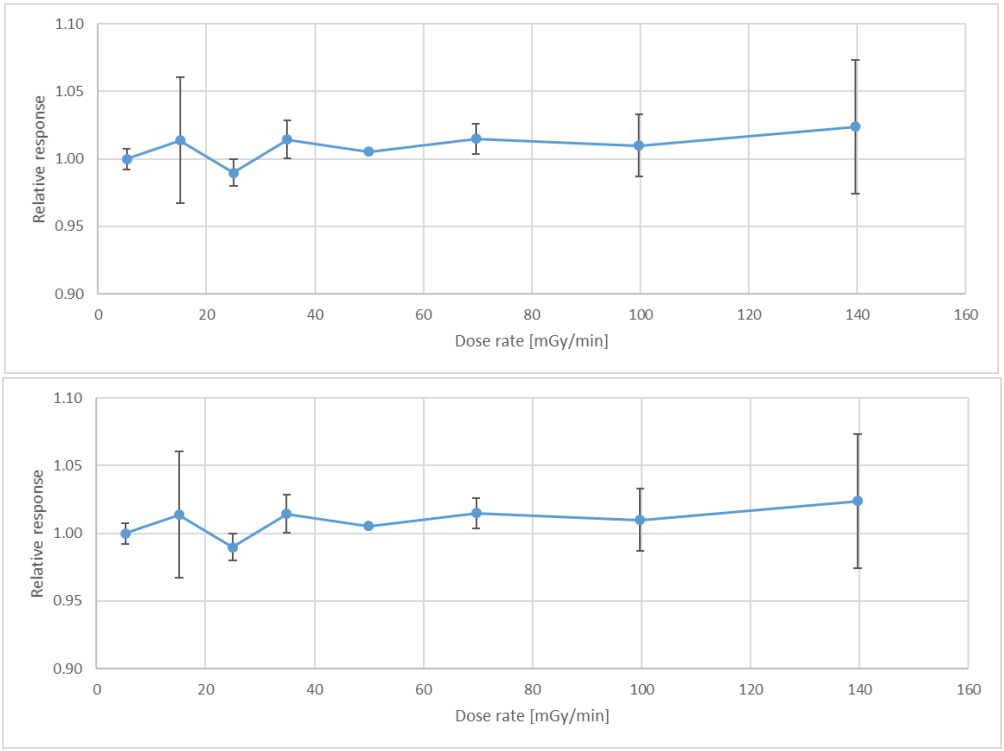

Figure 10: Dose rate dependence of LiF:Mg,Cu,P TLDs (MCP-N) normalized to the response at 5 mGy/min using RQR8 beam quality. Each point represents the average of three dosimeter response; error bars are the standard deviation of three dosimeter response.

The results of the study of the angular dependence of LiF:Mg,Cu,P TLDs (MCP-N), for incident angles up to (-) 90°, is presented in Figure 11 and 12 for RQR-8 (both figures) and VERIDIC3 80AlCu and VERIDIC2 120Al beams, respectively. Response was normalized to the response at 0°. For all angles and beam qualities, the response was within [-10%; 4%]; while the response was narrower and within ±4% for angles between 0 and 60°, which is of the same order of magnitude as the standard deviation of the three TLDs of a same set.

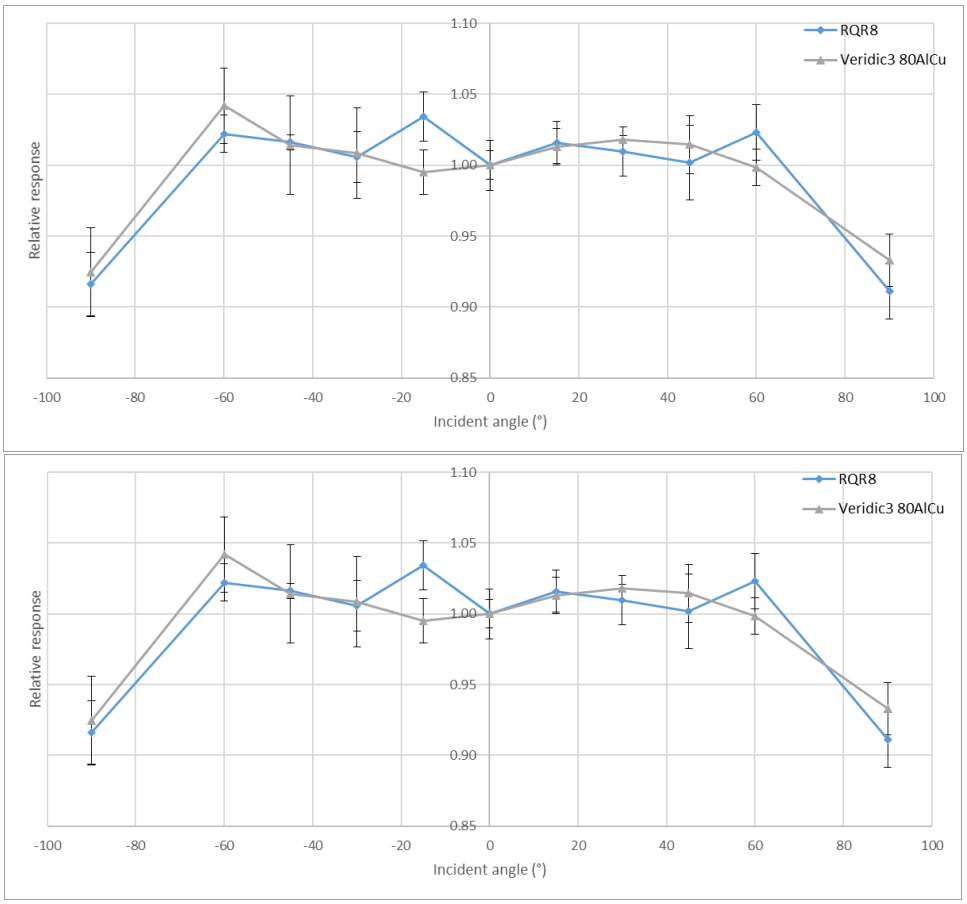

Figure 11: Angular dependence of LiF:Mg,Cu,P TLDs (MCP-N) normalized to the response at 0° (TLD pellet surface perpendicular to the incident beam). Energy dependence was investigated using RQR-8 and VERIDIC3 80AlCu beam qualities. Each point represents the average of three dosimeter response; error bars are the standard deviation of three dosimeter response.

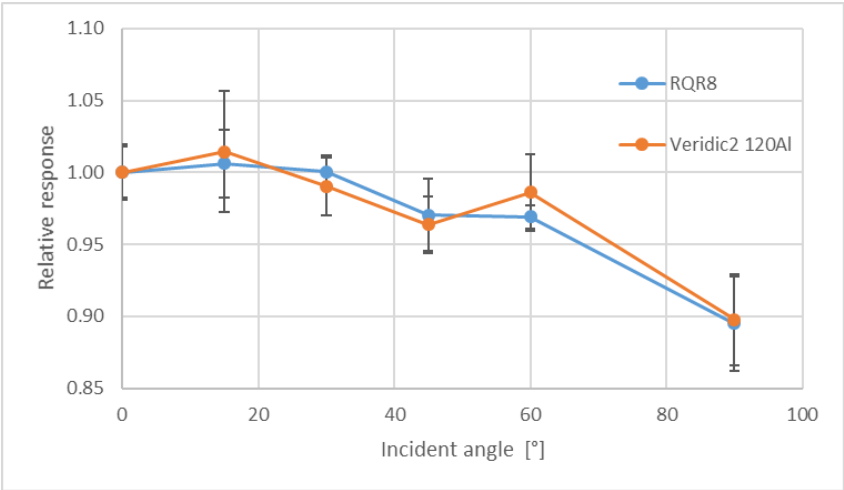

Figure 12: Angular dependence of LiF:Mg,Cu,P TLDs (MCP-N) normalized to the response at 0° (TLD pellet surface perpendicular to the incident beam). Energy dependence was investigated using RQR-8 and VERIDIC2 120Al beam qualities. Each point represents the average of three dosimeter response; error bars are the standard deviation of three dosimeter response.

In Figure 13, the relative response of LiF:Mg,Cu,P TLDs (MCP-N) is presented for RQR-8, VERIDIC1 80Al, VERIDIC2 120Al, VERIDIC3 80AlCu and VERIDIC4 120AlCu. Response is normalized to the response to Cs-137 for the present work. Results of other measurements using MCP-N TLDs (Olko 2002) are also plotted for comparison purpose. Very good agreement is observed.

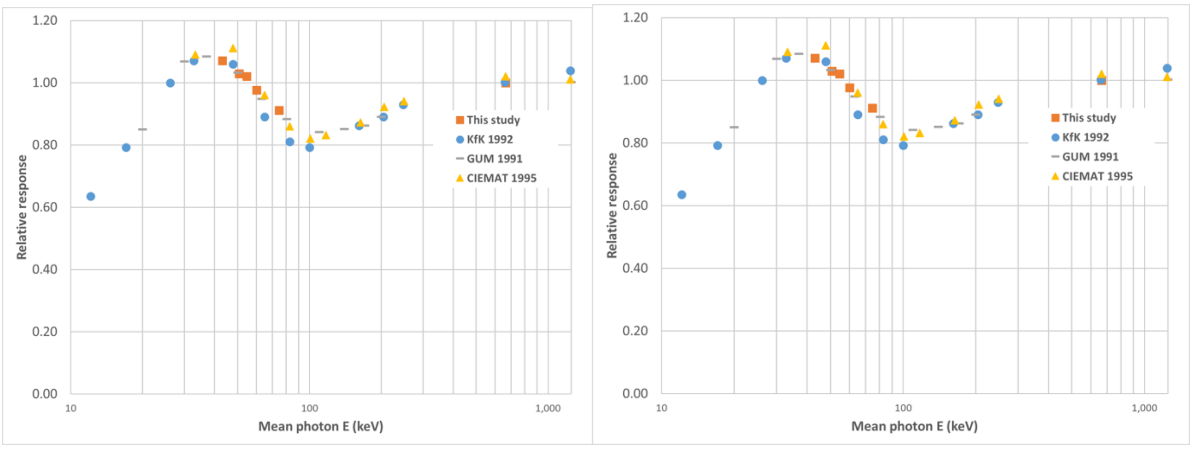

Figure 13: Energy dependence of LiF:Mg,Cu,P TLDs (MCP-N) from various studies. Response is normalized to the response to Cs-137 (current study (orange squares) and (blue circles) or to the response to Co-60 ((grey bars) and (yellow triangles)).

In Figure 14, the response to the different beam qualities are presented when one of the beam qualities (RQR-8 or one of the four VERIDIC beam qualities) is used for calibrating the TLDs. Responses are relative to the delivered dose. For example, the 5 first bars are the relative responses to RQR8, VERIDIC1, VERIDIC2, VERIDIC3 and VERIDIC4, respectively, when RQR-8 is used for calibrating the dosimeters. To limit the uncertainty associated with the energy dependence of the dosimeters, the calibration quality resulting in the smallest extent (i.e. the difference between the minimum and the maximum) of relative response and centered around one should be used. From a visual inspection, it appears that the extent of the relative response is nearly identical irrespective of the beam quality used for calibration. However, using beam qualities such as VERIDIC1 80Al or VERIDIC4 120AlCu would lead to systematic underestimation or overestimation of the dose in most cases, as well as to the highest underestimation and overestimation, respectively. The relative responses when using other beam qualities (RQR8, VERIDIC2 120Al and VERIDIC3 80AlCu) for calibration are better centered around 1 and therefore appear to be more adequate.

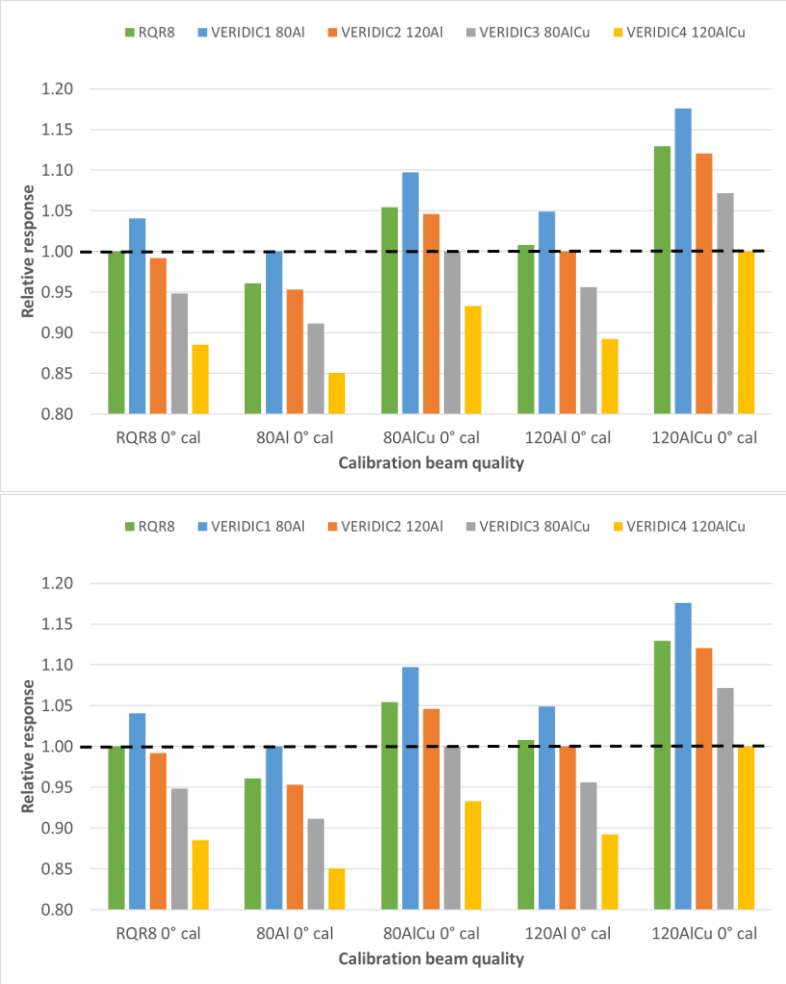

Figure 14: Energy dependence of LiF:Mg,Cu,P TLDs (MCP-N) calibrated with RQR-8 or one of the four VERIDIC beam qualities. Each color is the response to a specific beam quality; each group of 5 vertical bars is the response to different beam qualities when a specific beam quality is used for calibrating the dosimeters.

The energy dependence of LiF:Mg,Cu,P is the dominant source in the uncertainty budget of skin dose measurements. Therefore, selecting a proper calibration quality representative of the highly filtered beam used in IC is crucial. Without specific knowledge of the beams used during the IC procedures to be monitored, a uniform distribution of beam energies between the beams presented in the current work (VERIDIC beams and RQR8) can be assumed. The standard deviation of the energy response can be calculated as $\frac{(b-a)}{\sqrt{12}}$, where *b* and *a* are the maximum and the minimum responses, respectively. Applying that equation, a standard deviation of 5% is obtained. It should be noted that the influence of the scattered radiation spectrum, which has a reduced mean energy compared to the incident radiations[1], is not taken into account in that value. Although the additional uncertainty caused by the backscattered radiations is difficult to quantify, it is likely to be limited because (i) backscattered radiations contribute to a limited increase of the dose delivered by the primary beam at the entrance surface (between 0 and 80% on a 15 cm thick water phantom for various field size and photon energies encountered in IC (Benmakhlouf et al. 2013)) and (ii) the calibration beam VERIDIC2 has a mean energy (60 keV) which is centrally located in the

[1] According to Aoki and Koyama (2002), the mean energy of the backscattered spectrum is between 6 and 17% lower than the incident beam.

TLD energy response curve (Figure2b) for mean energies between 20 and 100 keV, thus possibly limiting the under-response to lower energies.

The angular dependence of LiF:Mg,Cu,P is the second most important uncertainty source, with under-response up to 10% for perpendicular exposure. Owing to the various angulations of the X-ray source during IC procedures, TLD can be exposed from virtually any direction. A uniform angle distribution can therefore be assumed, resulting in a standard uncertainty of 4%. For many IC procedures, however, the X-ray source is most frequently perpendicular to the patient back and the dosimeters (so-called posterior-anterior angulations), and angles greater than 45° are rarely used. Considering a uniform distribution over the range [-90°; 90°] is thus a conservative approach.

Considering the standard uncertainties (k=1) associated with the energy dependence (5%) and the angular dependence (4%) as determined in the current study, along with the characteristic uncertainties of the dosimetric system used (fading (3%), the individual sensitivity (2%), the repeatability (1%), the calibration coefficients (1.4%) and the calibration doses (2.2%)), an expanded uncertainty (k=2; 95% confidence interval) of 16% can be achieved for skin dose measurements in IC using LiF:Mg,Cu,P TLDs. Similar or lower uncertainty - thanks to their lower energy dependence - could be expected for LiF:Mg,Ti dosimeters provided their supralinear behavior is properly addressed.

If the position of the maximum skin dose to be measured is unknown, a correction factor as high as 40% and an additional uncertainty (possibly a standard deviation of 12%, depending the type of procedures and the number of dosimeters (Dabin et al. 2015)) should be used to account for the probability that no dosimeter might be in the region of the maximum skin dose.

Gafchromic films

XR-RV3 GafChromic films were used from the same lot number 01021901. An Epson Expression 12000 XL was used to scan these films, a model widely used and proven to have the required characteristics for accurate reading and analysis of Gafchromic™ films (H. Alnawaf et al.). The Epson Scan2 version 6.4 software was used for image analysis. Scanning was done in “Photo Mode”, reflective mode, without applying any adjustment or post processing option and with a resolution of 150 dpi. Each film was scanned orange side down in the most uniform area of the scanner (at the center). During scanning, 48-bit color images were acquired without adjusting the image itself or applying any post processing option. These images were saved in the .tif format as required by Film QA Pro 2016 version 5.0 (Ashland).

19 films cut in pieces of 3x3 cm^2 irradiated at different doses namely: 25, 50, 75, 100, 250, 400, 700, 850, 1000, 1500, 2000, 2500, 3000, 3500 and 5000 mGy were scanned jointly. In Film QA Pro, in the data Calibration module, a Region of Interest (ROI) of 1.5 cm x 1.5 cm in the center of the films was positioned. The red color channel was chosen and the mean measured reflective density was associated to the measured dose. The equation used was reciprocal linear versus dose as show in Figure 15. As shown in Farah et al. this type of equation reproduces at best the response of XR-RV3 films for high dose levels especially when a limited calibration range is used.

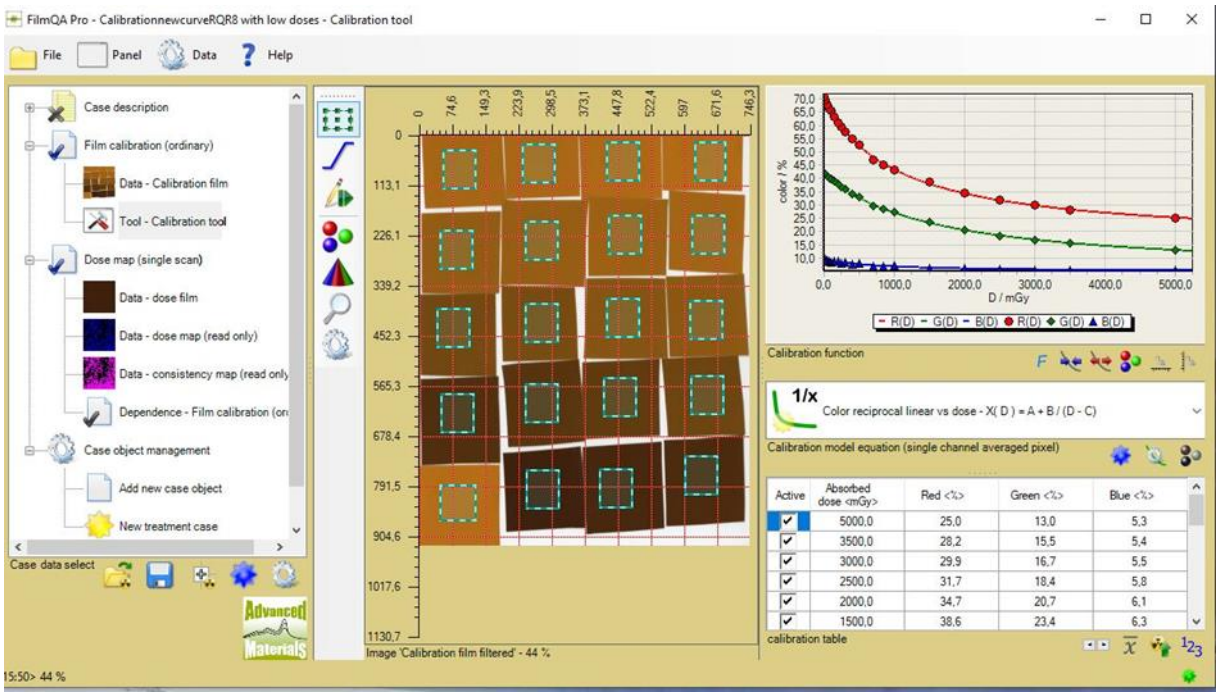

Figure 25 : Screenshot from FilmQA Pro showing the fitted equation for RQR8 calibration curve

The same procedure was repeated for each of the five different beam qualities in order to obtain a calibration curve per beam quality.

To reduce reading uncertainty, the same methodology was followed for all scanned films (QC or simplified procedure films). The readings were done with the red-light channel as it has been shown in many publications to be the most appropriate (maximum sensitivity and differentiation). An average reading of two scans was taken to minimize the variability between different scans.

In order to obtain MSD for each gafchromic film, a rectangular region of interest (ROI), of 1 cm^2 area, was placed in each film image by adjusting the axis in mm and selecting a dose area type of ROI. The 1 cm2 rectangular ROI was moved iteratively along the film until the maximum dose reading value was found which corresponds to the highest mean dose value obtained in the 1 cm^2 rectangle.

Uncertainty budget calculation using XR-RV3 Gafchromic films was used following the scenarios suggested by Farah et al. For all different steps except uncertainties related to film, the scenario A was used as the dose delivery was done in a primary calibration laboratory (CEA), and the methodology was followed closely with enough sampling. Scenario B was taken into account for the uncertainties related to film (Darkening over time, Film orientation, Humidity and temperature during transportation and storage) as the films could not be scanned at exactly the same number of days after irradiation, the orientation was not written on all films and most importantly they were sent through postal services. The uncertainty description and its estimate are provided in Table 4. Based on this uncertainty budget calculation, a standard uncertainty of 14% is therefore associated with the use of the Gafchromic films in Veridic project.

Uncertainty Description	Estimate (%)
Dose delivery uncertainty	
Air kerma rate measurements	0.8
Setup error and film positioning	0.1
Beam uniformity	0.3
Scanner-related uncertainty	
Scan uniformity	0.3
Short term stability	0.1
Long term stability	1.5
Scanner readout warm-up and software effects	-
Uncertainties related to a film	
Inter/intrabatch uniformity	4
Darkening over time	1.5
Effect of scan light	1
Dose rate dependence	3
Radiation quality dependence	10
Film orientation	6
Humidity and temperature during transportation and storage	2
Uncertainties related to calibration	
Fitting equation	2
Dose range of calibration points	2
Number and distribution of data points	2
Reading outliers and precision of fit parameters	3
Relative combined standard uncertainty (k=1)	14
Relative expanded uncertainty (k=2)	28

Table 4: Uncertainty Budget Calculation for XR-RV3 Gafchromic films

As calibration curves were also done another lot of Gafchromic XR-RV3: an old lot kept as back-up, it was interesting to compare the results for one beam quality namely RQR8.

GE MSD (mGy)	RQR8 (Old Lot)	RQR8(New Lot)	COV (%)
Procedure 1	530	465	9.2
Procedure 2	565	492,9	9.6
Procedure 3	520	466,9	7.6

Table 5: Comparison between two lots of Gafchromic films for GE equipment and RQR8 beam quality

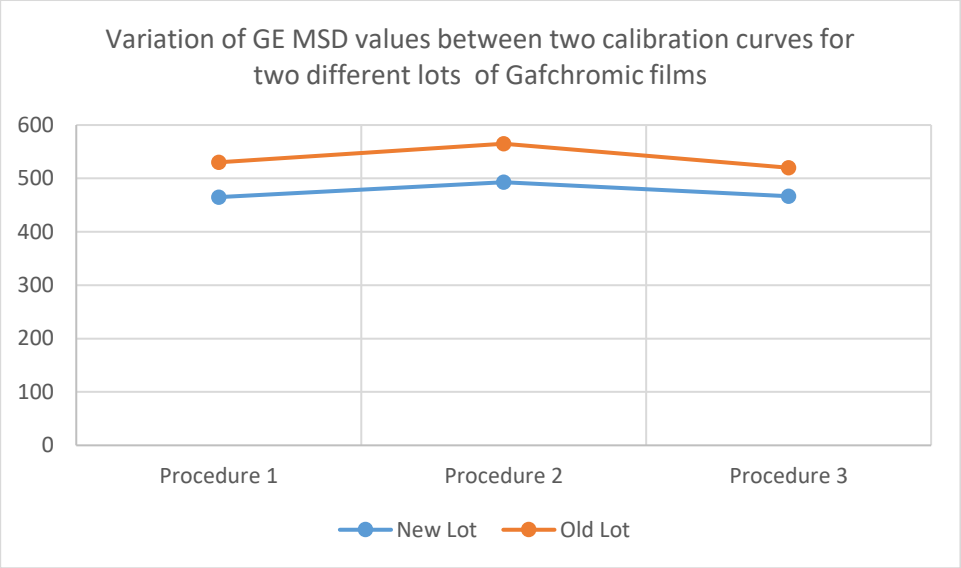

Figure 16: Variation of MSD values between two calibration curves reading for two different lots and GE equipment

COV was around 8-9% which is quite acceptable and indicated that it might be possible when accounting for it in the budget uncertainty to use the same calibration curve for another lot of film especially that the calibration of Gafchromic films at a primary or secondary standard dosimetry laboratory can be cumbersome (cost and time consuming).

As Gafchromic films are known to suffer from energy dependence (5), MSD could be over or under estimated depending on the beam quality that was used during the clinical procedure and how different this is from the calibration beam quality.

Therefore, coefficient Of Variation (COV) computed as standard deviation/mean was calculated for the difference of MSD between the 5 calibration curves (5 different beam quality) for three different simplified procedures and the four different manufacturers. The different MSD per manufacturer and beam quality is summarized in the tables 6-9.

Table 6: MSD for 5 different beam qualities for three simplified procedures on Philips equipment

Philips MSD (mGy)	RQR8	Veridic 80Al	Veridic 120 Al	Veridic80AlCu	Veridic 120AlCu	COV (%)
Procedure 1	281	372	325	280	255	17
Procedure 2	246	294	280	220	206	15
Procedure 3	275	290	272	219	205	15

Table 7 MSD for 5 different beam qualities for three simplified procedures on Canon equipment

Canon MSD (mGy)	RQR8	Veridic 80Al	Veridic 120 Al	Veridic80AlCu	Veridic 120AlCu	COV (%)
Procedure 1	886	981	920	739	707	14
Procedure 2	964	1006	860	685	657	19
Procedure 3	824	915	840	668	637	15

Table 8 MSD for 5 different beam qualities for three simplified procedures on Siemens equipment

Siemens MSD (mGy)	RQR8	Veridic 80Al	Veridic 120 Al	Veridic80AlCu	Veridic 120AlCu	COV (%)
Procedure 1	437	487	450	336	327	18
Procedure 2	510	595	509	412	359	19
Procedure 3	530	621	440	439	405	18

Table 9 MSD for 5 different beam qualities for three simplified procedures on GE equipment

GE MSD (mGy)	RQR8	Veridic 80Al	Veridic 120 Al	Veridic80AlCu	Veridic 120AlCu	COV (%)
Procedure 1	341	530	456	370	349	20
Procedure 2	493	560	501	377	360	19
Procedure 3	467	561	479	386	358	18

COV oscillated between 14 and 20% for the three simplified procedures and the 4 manufacturers.

The variation of MSD according to different calibration curves is illustrated in figures X-Y for all 4 manufacturers.

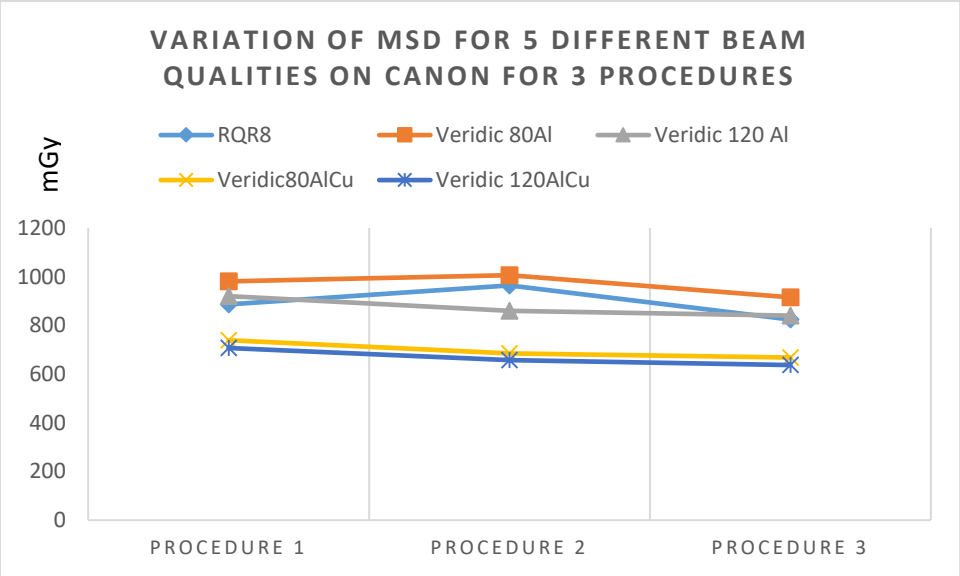

Figure 17 : Variation of MSD for 5 different beam qualities on Canon equipment

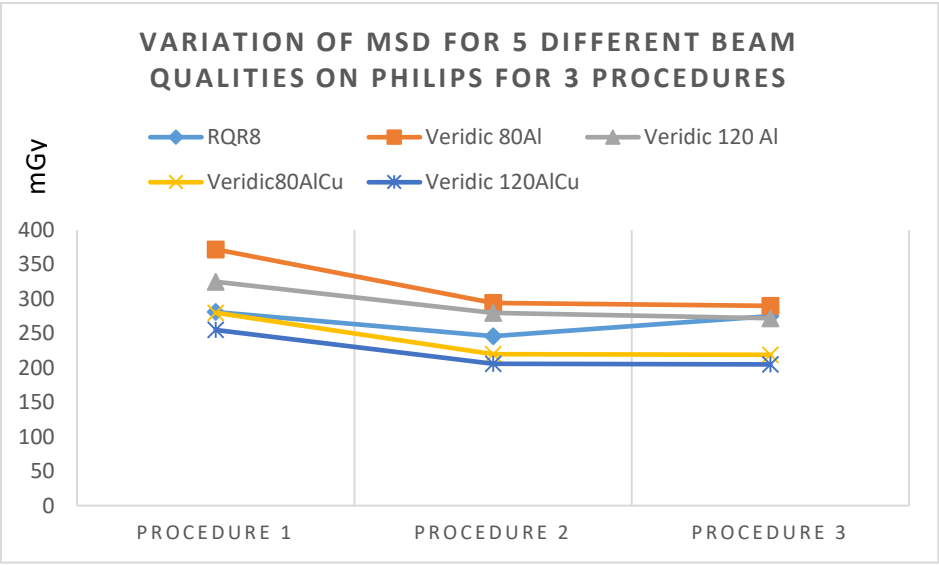

Figure 18: Variation of MSD for 5 different beam qualities on Philips equipment

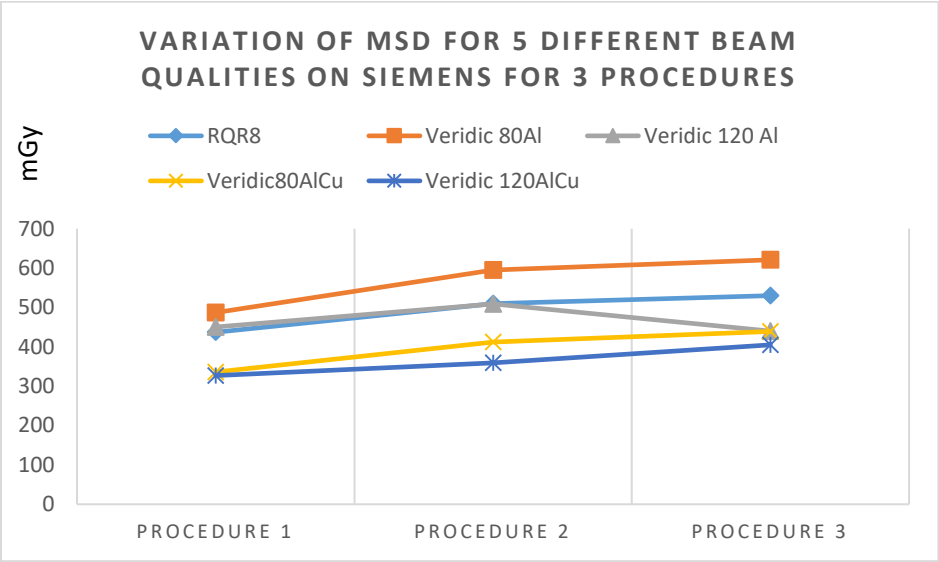

Figure 19: Variation of MSD for 5 different beam qualities on Siemens equipment

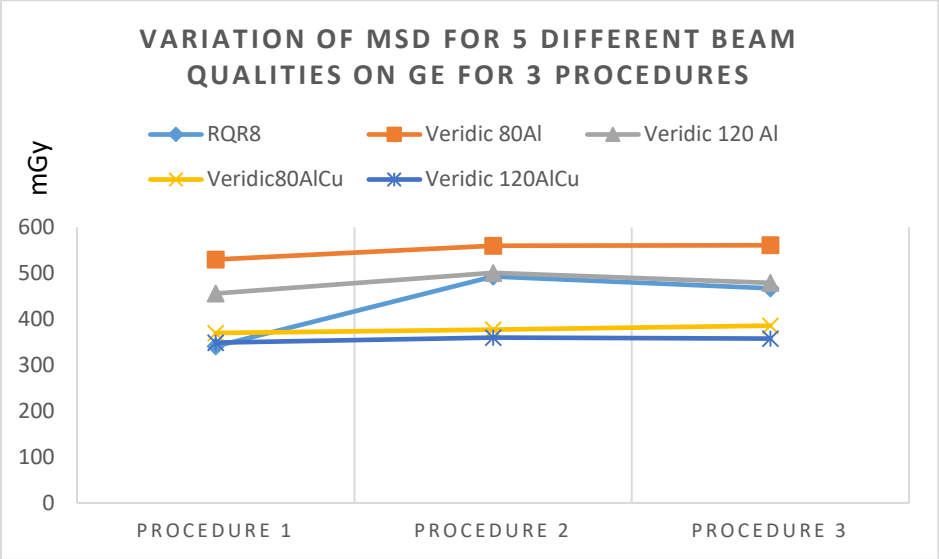

Figure 20: Variation of MSD for 5 different beam qualities on GE equipment

From Figures 17-20, With the same added filtration, the dose decreases with higher beam energy and that is observed for all manufacturers. For instance, MSD for procedure 1 for GE is 530 mGy using Veridic 80Al calibration curve and 456 mGy using Veridic 120Al beams. This has been shown by McCabe et al. as for the same filtration, exposing the film to 500 cGy at 100 kVp will yield 450 cGy at 120 kVp (reduction of 10%) or 600 cGy at 80 kVp (increase of 20%).

With added 0.904 mm Cu filtration the measured dose decreases when compared to only Al filtration. This is in line with the findings of Greffier et al. where the measured dose is underestimated with added filtration. For instance, MSD for procedure 1 for GE is 530 mGy using Veridic 80 Al calibration curve and 370 mGy using Veridic 80AlCu. In the same way, MSD for procedure 1 for GE is 456 mGy using Veridic 120Al calibration curve whereas MSD for procedure 1 is 349 mGy using Veridic 120AlCu calibration curve.

Quality control dosimeters calibrated using secondary standard at VINCA

Diagnostic dosimeters should be in compliance with IEC 61674 standard, which applies both to dosimeters equipped with ionization chambers and to semiconductor detectors. The dosimeters are routinely calibrated at the following standard radiation qualities (reference beam qualities according to IEC 61267): RQR2 (40 kV) – RQR10 (150 kV) which are not necessarily representative of the ones used clinically. The performance testing of x-ray equipment often requires the assessment of doses and dose rates for x-ray beams with many different radiation qualities and in non-standard conditions. The combination of different energy and angular distribution of radiation will influence detector performances in different x-ray fields, and could lead to significant differences in air kerma measurements. If different dosimeters are to be used in diagnostic radiology, users must understand what is being recorded and how the measurements are influenced by the detector characteristics. Therefore, the performance of dosimeters needs to be investigated, both in standard and non-standard conditions.

The performance testing of solid-state based radiation detectors used for acquisition of dosimetric data in the area of diagnostic radiology was executed in the Secondary Standard Dosimetry Laboratory (SSDL) of Vinca Institute of Nuclear Sciences, Serbia. The SSDL employs various secondary standard ion chambers for radiation protection, diagnostic radiology and radiotherapy (IAEA, 1999). Air-kerma rate was measured at the reference source to point-of-test distance of 100 cm, for one standard radiation quality and four non-standard radiation qualities, which correspond to the medical application X-ray fields. The standard radiation quality is established according to the recommendations of the International Atomic Energy Agency document TRS 457, regarding the calibrations of the dosimeters used for diagnostic radiology measurements (IAEA, 2007). The active dosimeter performance tests performed for standard and non-standard radiation qualities include energy dependence test, angular dependence test and the linearity test. The diagnostic dosimeter models tested are MPD and R100B (manufactured by RTI Electronics, used with the Barracuda multimeter unit), Piranha (manufactured by RTI Electronics), and Unfors Xi (manufactured by RaySafe). The chosen normalized radiation quality for which routine dosimeter calibration of diagnostic radiology instrumentation is performed in laboratory conditions is the RQR8 radiation quality (IAEA, 2007). The non-standard radiation qualities adapted to the clinical beam conditions were designed in a way that different primary photon beam filtration has been employed along with the X-ray tube voltages similar to the value used in establishing the standard quality. The radiation qualities' properties are displayed in Table 10.

Radiation Quality	X-ray tube voltage [kV]	Half-value layer [mm Al]	Additional filtration [mm Cu]	Calibration coefficient [mGy nC^{-1}]
RQR8	100	3.97	/	7.971
R80_0	80	2.55	0	8.505
R80_09	80	8.63	0.9	8.482
R120_0	120	3.73	0	8.513
R120_09	120	11.33	0.9	8.526

Table 10: Radiation quality properties used for performance testing of diagnostic radiology solid-state dosimeters.

The inherent filtration for 80 kV and 120 kV non-standard radiation qualities was 2.5 mm Al, and the qualities termed as R80_09 and R120_09 were established by adding a 0.9 mm Cu layer to the inherent filtration. The reference air-kerma rate values were measured by using the 3.6 cm^3 spherical diagnostic reference level ionization chamber (A3, Exradin), whose calibration coefficients are presented in Table 4, for standard and non-standard radiation qualities. All of the air-kerma rate measurements were corrected for the influence of ambient conditions (air density, including ambient temperature and pressure, while the influence of relative humidity can be neglected), and for the small variations of the X-ray generator output. The X-ray generator output correction is determined by measuring the collected charge with a standard monitoring ionization chamber (PTW 34014), during the measurements with the reference ionization chamber and the solid-state detectors.

The effect of influence quantity of photon energy on the measurement result is an important dosimetric characteristic, that needs to be accounted for when performing measurements in various radiation fields that may greatly differ from the reference radiation quality beam parameters under which the instrument has been calibrated in the laboratory conditions. In this research the influence of photon energy of four solid-state detectors has been tested depending of the half-value layer of the X-ray beams. Due to the difference in the photon spectra after the filtration of the primary beam, the mean energy of the filtered beam can be related to the half-value layer of the radiation quality. The energy dependence test results are estimated in terms of relative response of the dosimeter. Reference absolute response value has been determined for the RQR8 standard radiation quality. The relative response is determined by using the following equation:

$$r = \frac{R}{R_0} = \frac{M/(Q \cdot N_K \cdot k_D \cdot k_M)}{R_0}$$

where R and R_0 are the absolute response values for the non-standard radiation qualities and the standard (reference) radiation quality, respectively. The absolute dosimeter response is defined as the quotient of the value M indicated by the solid-state detector, and the reference value of air-kerma rate defined by the term $Q \cdot N_K \cdot k_D \cdot k_M$, which includes collected charge in the active volume of the ionisation chamber, the ionization chamber calibration coefficient, the air density correction factor and the monitor chamber correction factor for the X-ray generator output, respectively.

The influence of angle of incidence on the indication of the solid-state detectors was tested for the standard RQR8 radiation quality, and the non-standard R80_09 radiation quality. The range of influence quantity angle of incidence was from 0° to ±90°, with an increment of 15°. The relative angular dosimeter response was determined by normalizing the measured absolute response values with the value acquired for the 0° angle of incidence, for each radiation quality independently.

The linearity performance test has been performed for the normalized RQR8 and non-standard R80_09 radiation qualities. Solid-state detectors were irradiated in these X-ray fields of different air-kerma rates, achieved by varying the X-ray tube current values in range from 3 mA up to 25 mA. The linearity test results were expressed as the normalized dosimeter response to the reference air-kerma rate value chosen for the tube current of 9 mA, for each of the radiation qualities separately.

The performance test results of solid-state active dosimeters for diagnostic radiology are displayed in Figures 21-25. Energy dependence of the dosimeter response, in terms of HVL dependence is displayed in Figure 21, by normalizing the relative response values to the absolute response measured for RQR8. Figures 22 and 23 contain results of the angular dependence test for the RQR8 and R80_09 radiation qualities, respectively. Figures 24 and 25 display the linearity test results for the RQR8 and R80_09 radiation qualities.

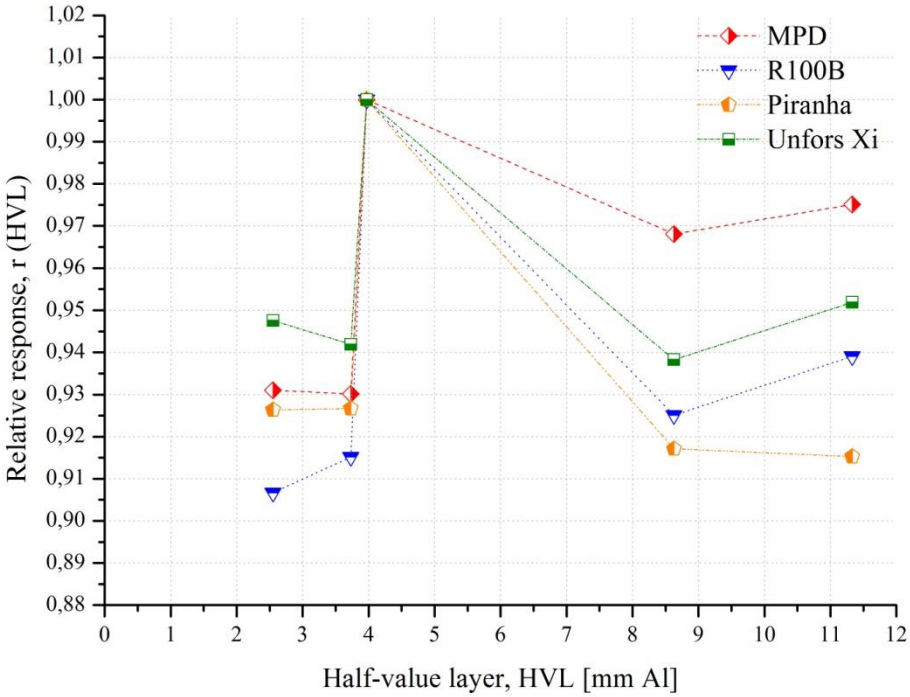

Figure 21: Relative response of four solid-state detectors measured for one normalized radiation quality (RQR8) under laboratory conditions, and the four non-standard radiation qualities which correspond to the clinical conditions (R80_0, R120_0, R80_09 and R120_09).

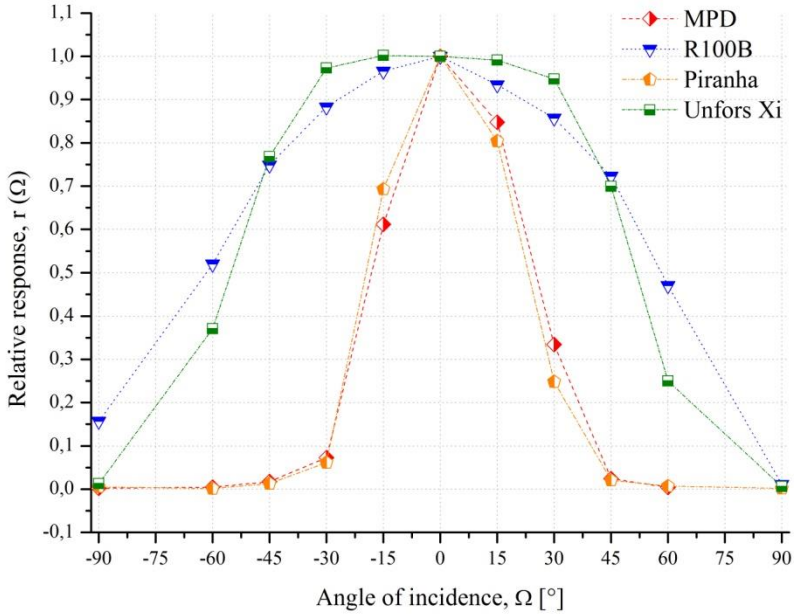

Figure 22: The angular dependence test results of four solid-state detectors for the normalized RQR8 radiation quality, in the angle range from 0° to ±90°. The relative angular response has been normalized to the 0° absolute response value.

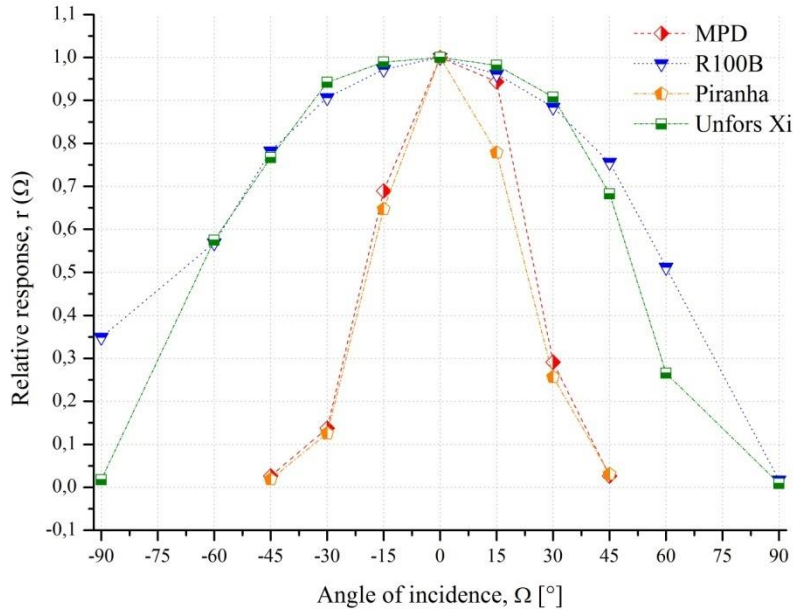

Figure 23: The angular dependence test results of four solid-state detectors for the non-standard R80_09 radiation quality, in the angle range from 0° to ±90°. The relative angular response has been normalized to the 0° absolute response value.

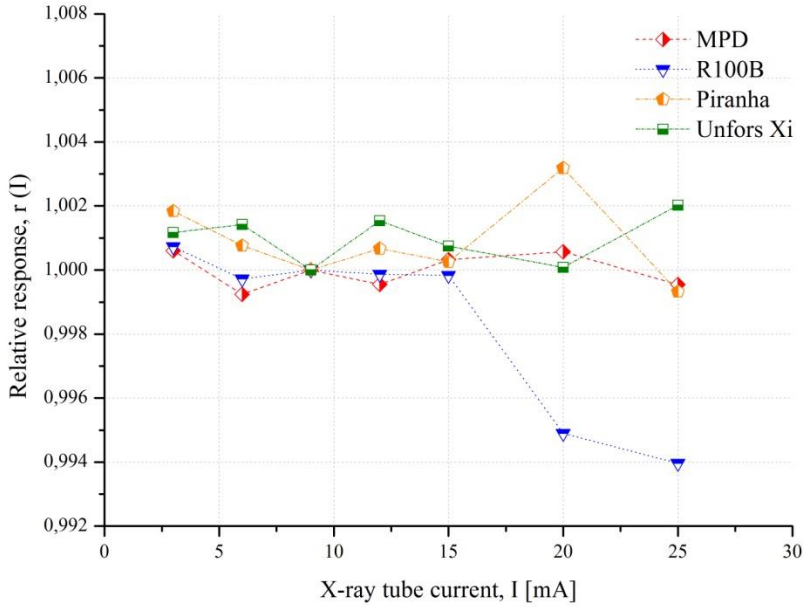

Figure 24: The linearity test results for four solid-state detectors in the air-kerma rate range determined by the X-ray tube current range from 3 mA to 25 mA, for the normalized RQR8 radiation quality. The relative response has been normalized to the absolute response value at 9 mA X-ray tube current.

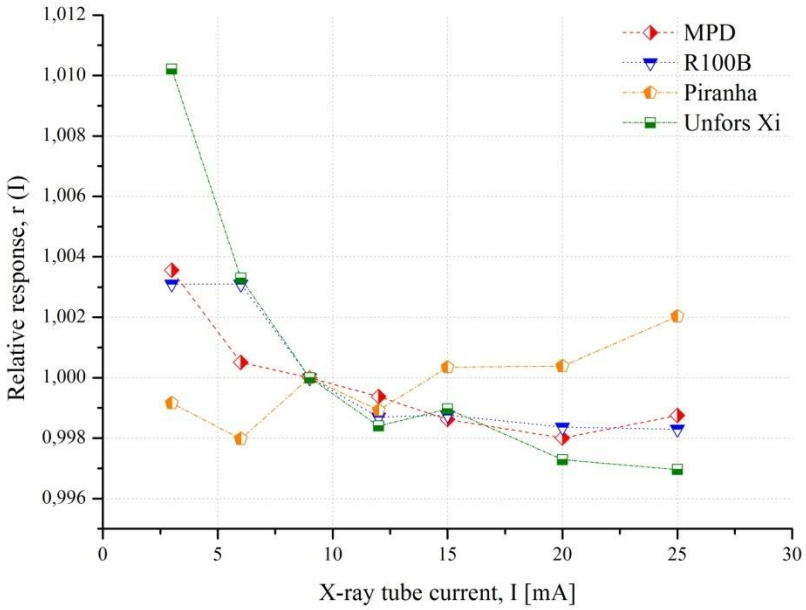

Figure 25: The linearity test results for four solid-state detectors in the air-kerma rate range determined by the X-ray tube current range from 3 mA to 25 mA, for the non-standard R80_09 radiation quality. The relative response has been normalized to the absolute response value at 9 mA X-ray tube current.

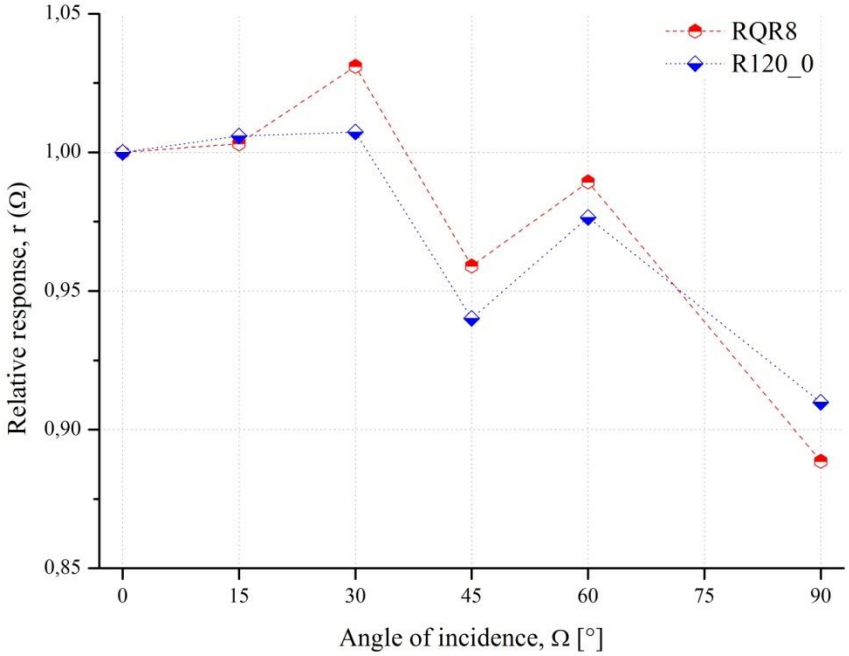

Figure 26: Angular dependence test results of thermoluminescent dosimeters expressed in terms of relative angular response for the normalized RQR8 and non-standard R120_0 radiation qualities, for the angle of incidence ranging from 0° to 90°, where the absolute responses were normalized for each radiation quality separately.

Conclusions

Four new reference beam qualities relevant for interventional cardiology have been established and metrologically characterized in terms of air kerma rate using dedicated primary standards available at CEA. These new standards allowed accurate calibration and extensive study for different types of dosimeters, the most suitable for this application, both active (solid state, ionization chamber) and passive (TLD, Gafchromic films).

The calibration and testing of dosimeters used for QC in diagnostic and interventional radiology was performed under, and pertains to, standard and non-standard beam qualities. When in use, the dosimeter is operated under non-reference conditions, where the influence quantities may have values deviating from their reference values. The results of testing have confirmed that the energy dependence of the response of a dosimeter should be considered in dose measurement and appropriate corrections can be applied. Energy response of tested dosimeters varied up to 10% in the range of HVL from 2.55 to 11.3 mm Al and tube voltages of 80 kV and 120 kV. Calibration at only one radiation quality (e.g. RQR 8, 100 kV) might be insufficient for highly energy dependent dosimeters, as calibration coefficient can vary up to 7%. Different dose rates, commonly used in image acquisition modalities in interventional procedures, did not affect significantly the response of a dosimeter. The dosimeters being tested in this study showed good performance in terms of linearity. This is in line with the IEC standard, which requires dose measurement with less than 5% error. Therefore, a dosimeter that complies with IEC standards and operates according to its specifications could be used at typical clinical exposures conditions taking into account only corrections for the energy dependence of response. However, it is recommended to perform detailed tests in the clinical beam qualities, if these are significantly different from standard ones.

Among all possible solutions, film dosimetry represents the most convenient method to determine skin dose. A comprehensive evaluation in order to investigate the optimal use of films in the interventional

environment has been performed elsewhere (Farah at al. 2015a, Farah at al. 2015b, EURADOS 2018). The reliability and applicability of GafChromic films for quantitative estimates of skin dose in interventional radiology and cardiology is directly related to film properties and performance in clinical conditions. Scanner-related uncertainty analysis showed that multiple scanner models and types can be used for such dosimetry applications, with an overall scanner-related uncertainty in a range from 2 % to 7 % at one standard deviation. It has been proved that showed that XR-RV3 films have good uniformity within one batch (up to 1.6 %), continue to darken with time after exposure for up to 24 hours and have a dependence on dose rate of 4.5 %. Radiation quality and film orientation were highlighted as the main sources of film-related uncertainties with up to 15 % and 10 % impact on film darkening, respectively. It is therefore crucial to choose an appropriate calibration beam energy depending on the performance and capacities of the x-ray system used clinically prior to conducting patient skin dose measurements, whereas the overall film-related uncertainty was estimated to range from 6% to 19 % (k=1). Finally, fitting uncertainties were found to be the main source of uncertainty when determining skin dose using XR-RV3 GafChromic films. Nonetheless, with properly selected calibration curve, this uncertainty can be well controlled. Depending on the level of control of different dosimetry steps, the overall skin dose uncertainty may range from 12 to 62 %.

LiF:Mg,Cu,P TLDs showed limited variation in their response to the new beam qualities. The energy dependence remained nevertheless the dominant uncertainty source for skin dose measurements (5%, k=1). The angular dependence of LiF:Mg,Cu,P was the second most important uncertainty source, with under-response up to 10% for perpendicular exposure (4%, k=1). Considering all uncertainties associated with skin dose measurements as determined in the current study and as per the literature, an expanded uncertainty (k=2; 95% confidence interval) of about 16% can be achieved for skin dose measurements in IC using LiF:Mg,Cu,P TLDs. However, if the position of the maximum skin dose to be measured is unknown, the additional uncertainty arising from the limited spatial coverage of the TLDs become dominant over all other sources.

References

G. Poludniowski et al., SpekCalc: a program to calculate photon spectra from tungsten anode x-ray tubes, *Phys. Med. Biol.* 54 N433 (2009)

J. Plagnard, Comparison of measured and calculated spectra emitted by the X-ray tube used at the Gustave Roussy radiobiological service, X-Ray Spectrometry 43, Issue 5, 298-304 (2014)

Wassim Ksouri, Étude et réalisation des références dosimétriques nationales en termes de kerma dans l'air pour les faisceaux de rayons X de basses et moyennes énergies. Physique Nucléaire Expérimentale [nucl-ex]. Université de Nice-Sophia Antipolis, 2008. Français. NNT : 2008NICE4107 . tel-02272150

Aoki, K. and Koyama M. 2002. Measurement of backscattered x-ray spectra at the water surface in the energy range 60 kV to 120 kV. Phys Med Biol 47(7): 1205-1217.

Benmakhlouf, H. et al. (2013). Influence of phantom thickness and material on the backscatter factors for diagnostic x-ray beam dosimetry. Physics in Medicine & Biology 58(2): 247.

Bilski, P., et al. 2013. Thermoluminescence fading studies: Implications for long-duration space measurements in Low Earth Orbit. Radiation Measurements 56: 303-306.

Bogaert E., Bacher K., Lemmens K., Carlier M., Desmet W., De Wagter X., et al. 2009. A large-scale multicentre study of patient skin doses in interventional cardiology: dose-area product action levels and dose reference levels. Br J Radiol.,82:303-12.

Burgkhardt, B., R. Herrera and E. Piesch 1978a. The effect of post-irradiation annealing on the fading characteristic of different thermoluminescent materials part I — experimental results. Nuclear Instruments and Methods 155(1): 293-298.

Burgkhardt, B. and E. Piesch 1978b. The effect of post-irradiation annealing on the fading characteristic of different thermoluminescent materials part II — optimal treatment and recommendations. Nuclear Instruments and Methods 155(1): 299-304.

Carinou, E., et al. 2008. Energy dependence of TLD 100 and MCP-N detectors. Radiation Measurements 43(2-6): 599-602.

Carinou, E., et al. 2011. Pre- and post-irradiation fading effect for LiF:Mg,Ti and LiF:Mg,Cu,P materials used in routine monitoring. Radiat Prot Dosimetry 144(1-4): 207-210.

Cassata, J. R., Moscovitch, M., Rotunda, J. E. and Velbeck, K. J. 2002. A new paradigm in personal dosimetry using LiF:Mg,Cu,P. Radiat. Prot. Dosim. 101, 27–42.

Ciraj Bjelac O., J. Dabin, J. Farah, H. Järvinen, F. Malchair, T. Siiskonen, Ž. Knežević: Patient maximum skin dose in interventional procedures in radiology and cardiology: summary of WG 12 activities, EURADOS Report 2019-02, EURADOS, 2019

Dabin, J., et al. 2015. Characterisation of grids of point detectors in maximum skin dose measurement in fluoroscopically-guided interventional procedures. Physica Medica-European Journal of Medical Physics 31(8): 1112-1117.

Dabin J., Maeremans J., Berus D., Schoonjans W., Tamborino G., Dens J., Kayaert, P. 2018 Dosimetry during Percutaneous Coronary Interventions of Chronic Total Occlusions. Radiat Prot Dosimetry.

Davis, S. D., et al. 2003. The response of lif thermoluminescence dosimeters to photon beams in the energy range from 30 kV x rays to 60Co gamma rays. Radiat Prot Dosimetry 106(1): 33-43.

Didier R, Bourhis D, Oueslati C, Nasr B, Le Ven F, Noël A, Jobic Y, Damien P, Pene-Baverez D, Mansourati Nicol, J. PP, Gilard M. In vivo validation of Dosemap software use in interventional cardiology with dosimetrics indicators and peak skin dose evaluation. Catheter Cardiovasc Interv. 2019, 94: 216-222. Duggan, L. and T. Kron 1999. Glow Curve Analysis of Long-term Stability of LiF:Mg,Cu,P as Compared to LiF:Mg,Ti. Radiation Protection Dosimetry 85(1-4): 213-216.

Duggan, L. et al. 2004. Variations in dose response with x-ray energy of LiF:Mg,Cu,P thermoluminescence dosimeters: implications for clinical dosimetry. Physics in Medicine & Biology 49(17): 3831.

Farah J., Trianni A., Ciraj-Bjelac O., Clairand I., De Angelis C., Delle Canne S., Hadid L., Huet C., Jarvinen H., Negri A., Novák L, Pinto M., Siiskonen T., Waryn MJ., Knežević Ž. 2015a Characterization of XR-RV3 GafChromicTM films in standard laboratory and clinical conditions and means to estimate uncertainties and reduce errors, Med. Phys. 42(7) 4211-26.Gamboa-deBuen, I., A. E. Buenfil, C. G. Ruiz,

M. Rodríguez-Villafuerte, A. Flores and M. E. Brandan 1998. Thermoluminescent response and relative efficiency of TLD-100 exposed to low-energy x-rays. Physics in Medicine & Biology 43(8): 2073.

Gilvin, P. J. 2007. Comparison of time effects, decision limit and residual signal in Harshaw LiF:Mg,Ti and LiF:Mg,Cu,P. Radiat. Prot. Dosim. 125, 233–236.

Greffier J, Van Ngoc Ty C, Bonniaud G, Moliner G, Ledermann B, Schmutz L, Cornillet L, Cayla G, Beregi JP, Pereira F. Assessment of peak skin dose in interventional cardiology: A comparison between Gafchromic film and dosimetric software em.dose. Phys Med. 2017 38, 16-22.

Habib Geryes B, Hadid-Beurrier L, Waryn MJ, Jean-Pierre A, Farah J. Benchmarking the DACS-integrated Radiation Dose Monitor® skin dose mapping software using XR-RV3 Gafchromic® films. Med Phys. 2018, 45:4683-4692. Harvey, J. A., N. P. Haverland and K. J. Kearfott 2010. Characterization of the glow-peak fading properties of six common thermoluminescent materials. Appl Radiat Isot 68(10): 1988-2000.

Horowitz, Y., 1990. Editorial: Fading in LiF:Mg,Ti. Radiat. Prot. Dosim.32,147.

Horowitz, Y., L. Oster and I. Eliyahu 2018. Review of dose-rate effects in the thermoluminescence of Lif:Mg,Ti (Harshaw). Radiat Prot Dosimetry 179(2): 184-188.

Hosseini-Pooya, M., Jafarizadeh, M. 2004. Effect of reader and oven annealing on the glow curve structure and fading of a LiF:Mg,Cu,P TL dosimeter. J. Radiol. Prot. 24,173–178.

Hranitzky, C., et al. 2006. Determination of LiF:Mg,Ti and LiF:Mg,Cu,P TL efficiency for X-rays and their application to Monte Carlo simulations of dosimeter response. Radiat Prot Dosimetry 119(1-4): 483-486.

Hourdakis, C. J., Boziari, A. & Manetou, A. Performance evaluation of diagnostic radiology dosimeters in clinical and calibration x-ray beams. Health Phys. 2010; 98, 704-716.

International Atomic Energy Agency (IAEA), "The IAEA/WHO Network of Secondary Standard Dosimetry Laboratories", IAEA, Vienna, 2018.

International Atomic Energy Agency (IAEA), "Dosimetry in Diagnostic Radiology: An International Code of Practice", Technical Report Series No. 457, IAEA, Vienna, 2007.

INTERNATIONAL ELECTROTECHNICAL COMMISSION, Medical Electrical Equipment – Dosimeters With Ionization Chambers and/or Semi-conductor Detectors as Used in X-ray Diagnostic Imaging, Report 61674, IEC, Genève (1997).

INTERNATIONAL ELECTROTECHNICAL COMMISSION, Medical Diagnostic X-ray Equipment – Radiation Conditions for Use in the Determination of Characteristics, Report 1267, IEC, Genève (2005).

Kron, T., et al. 1998. Dose response of various radiation detectors to synchrotron radiation. Physics in Medicine and Biology 43(11): 3235-3259.

Martin, C. J. An evaluation of semiconductor and ionization chamber detectors for diagnostic x-ray dosimetry measurements. Phys Med Biol. 2007; 52, 4465-4480.Massillon-Jl, G., I. Gamboa-deBuen and M. E. Brandan 2006. Onset of supralinear response in TLD-100 exposed to60Co gamma-rays. Journal of Physics D: Applied Physics 39(2): 262-268.

McCabe BP., Speidel MA., Pike TL., Van Lysel MS., 2011. Calibration of GafChromicTM XR-RV3 radiochromic film for skin dose measurement using standardized x-ray spectra and a commercial flatbed scanner, Med. Phys. 38(4) 1919-30

McKeever S W S, M Moscovitch and P D Townsend 1995 Thermoluminescence Dosimetry Materials. Properties and Uses (Ashford, UK: Nuclear Technology Publishing), pp 80–92

Moscovitch, M. and Y. S. Horowitz 2007. Thermoluminescent materials for medical applications: LiF:Mg,Ti and LiF:Mg,Cu,P. Radiation Measurements 41: S71-S77.

Nunn, A. A., et al. 2008. LiF:Mg,Ti TLD response as a function of photon energy for moderately filtered x-ray spectra in the range of 20–250 kVp relative to [sup 60]Co. Medical Physics 35(5): 1859.

Olko, P. 2002 Microdosimetric Modelling of Physical and Biological Detectors. Report 1914/D. Kraków, IFJ.

Roshau JN, Hintenlang DE. Characterization of the angular response of an "isotropic" MOSFET dosimeter. Health Phys. 2003 Mar;84(3):376-9.

Richley L., John AC., Coomber H., Fletcher S., 2010. Evaluation and optimization of the new EBT2 radiochromic film dosimetry system for patient dose verification in radiotherapy, Phys. Med. Biol. 55, 2601-2617.

Sáez-Vergara, J. C., et al. 1999. Photon Energy Response Matrix for Environmental Monitoring Systems Based on LiF:Mg,Ti and Hypersensitive Phosphors (LiF:Mg,Cu,P and a-Al2O3:C). Radiation Protection Dosimetry 85(1-4): 207-211.

Tse J, McLean D. Investigation of the clinical performance of a novel solid-state diagnostic dosimeter. J Appl Clin Med Phys. 2015;16(4):244–253.

H. Alnawaf, P. Yu, and M. Butson, “Comparison of Epson scanner quality for radiochromic film evaluation,” J. Appl. Clin. Med. Phys. 13(5), 314–321 (2012).

G. Thomas, R. Y. L. Chu, and E. Rabe, “A study of GafChromic® XR type R film response with reflective-type densitometers and economical flatbed scanners,” J. Appl. Clin. Med. Phys. 4, 307–314 (2003).

S. A. Dini, R. A. Koona, J. R. Ashburn, and A. S. Meigoonia, “Dosimetric evaluation of GafChromic® XR type T and XR type R films,” J. Appl. Clin. Med. Phys. 6, 114–134 (2005).

A. Blair and Y. Meyer, “Characteristics of GafChromic® XR-RV2 radiochromic film,” Med. Phys. 36(7), 3050–3058 (2009).

B. P. McCabe, M. A. Speidel, T. L. Pike, and M. S.Van Lysel, “Calibration of GafChromic® XR-RV3 radiochromic film for skin dose measurement using standardized x-ray spectra and a commercial flatbed scanner,” Med. Phys. 38(4), 1919–1930 (2011).

Farah J, Trianni A, Ciraj-Bjelac O et al. Characterization of XR-RV3 Gafchromic films in standard laboratory and in clinical conditions and means to evaluate uncertainties and reduce errors. Med Phys 2015; 42:4211-4226.

J. Greffier, C.vanNgocTy ,M.Agelou,J.Coulot ,B.Ledermann,et al. Impact of the calibration conditions of XR-RV3 films on peak skin dose measurements in interventional radiology. Radiation Protection Dosimetry,OxfordUniversityPress(OUP),2017,174(2),pp.207-215.